

KEYDIFF: Key Similarity-Based KV Cache Eviction for Long-Context LLM Inference in Resource-Constrained Environments

Junyoung Park¹ Dalton Jones¹ Matthew Morse¹ Raghav Goel¹ Mingu Lee¹ Chris Lott¹

Abstract

In this work, we demonstrate that distinctive keys during LLM inference tend to have high attention scores. We explore this phenomenon and propose KEYDIFF, a training-free KV cache eviction method based on key similarity. This method facilitates the deployment of LLM-based application requiring long input prompts in resource-constrained environments with limited memory and compute budgets. Unlike other KV cache eviction methods, KEYDIFF can process arbitrarily long prompts within strict resource constraints and efficiently generate responses. We demonstrate that KEYDIFF computes the optimal solution to a KV cache selection problem that maximizes key diversity, providing a theoretical understanding of KEYDIFF. Notably, KEYDIFF does not rely on attention scores, allowing the use of optimized attention mechanisms like FlashAttention. We demonstrate the effectiveness of KEYDIFF across diverse tasks and models, illustrating a performance gap of less than 0.04% with 8K cache budget ($\sim 23\%$ KV cache reduction) from the non-evicting baseline on the LongBench benchmark for Llama 3.1-8B and Llama 3.2-3B.

1. Introduction

Large language models (LLMs) have revolutionized natural language processing, enabling tasks like document summarization, code generation, question answering (Brown et al., 2020; Raffel et al., 2020; Touvron et al., 2023; Dubey et al., 2024). Many exciting applications of LLMs, such as retrieval augmented generation (Lewis et al., 2020) and reasoning tasks (Wei et al., 2022; Kojima et al., 2022; Yao et al., 2024), require very long input prompts, or *long context* support, to provide a valuable end-user experience. However, deploying these models in production environments has grown in importance and managing long input prompts

¹Qualcomm AI Research, San Diego, CA, USA. Correspondence to: Junyoung Park <junpark@qti.qualcomm.com>.

remains a challenge due to large compute and memory requirements.

Due to cost and privacy concerns, there has been a recent focus on deploying LLMs *on the edge*, i.e. directly on devices such as mobile phones or personal computers (Alizadeh et al., 2023; Liu et al., 2024c; van Baalen et al., 2024; Xu et al., 2024a). This imposes tight resource constraints, such as limited or shared compute resources, limited available DRAM, and even power limits in the mobile setting. Many techniques, such as system optimization (Alizadeh et al., 2023; Liu et al., 2024c; Xu et al., 2024a), model quantization (van Baalen et al., 2024), and efficient text generation (Goel et al., 2024) help to enable on-device LLM inference, but the main challenge for long context application on-device deployment is effectively managing key and value states.

In a naïve implementation of autoregressive text generation, key and value states (KVs) must be recomputed for each new generated token. In a decoder-only transformer model, one can instead store the previously computed KVs in a *KV cache* for later use, allowing for a significant decrease in LLM inference latency. This comes at the cost of maintaining the KV cache, whose memory footprint grows linearly with the input sequence length (Yang et al., 2024a) and will violate any imposed memory limit with a sufficiently large input.

One solution to bound this memory overhead is to fix the number of KVs in the cache, or *cache budget*, and use a *cache eviction policy* to remove KVs from the cache when the budget has been exceeded, bounding the KV cache memory usage. However, state-of-the-art cache eviction policies retain KVs with high attention weights (Xiao et al., 2024; Oren et al., 2024; Zhang et al., 2024b), which requires explicitly materializing the attention matrix of the entire input prompt. This results in large intermediate memory overhead during cache eviction, often violating memory limits.

This intermediate cache memory overhead can be mitigated by segmenting the input prompt into blocks, sequentially processing each block by the LLM and caching the intermediate KVs (Kwon et al., 2023; Agrawal et al., 2023; Xu et al., 2024b). The cache eviction policy can be applied block-wise to satisfy imposed memory constraints (Figure 1). However, our experiments show that applying existing attention-based

eviction methods with block prompt processing results in performance degradation of downstream tasks (Table 1). This is due to the limited scope of the attention computation during block prompt processing: attention scores are only computed for a subsequence of the original prompt and only contain local information. These partial scores may not be representative of a token’s global importance across the entire prompt and can result in incorrect cache eviction. This means that we need an eviction method that is independent from attention and cheap to compute during inference while maintaining model capability.

The “attention sink” phenomenon (Xiao et al., 2024; Sun et al., 2024) describes the observation that, in decoder-only transformer-based LLMs, high attention scores are assigned to the first few tokens in the KV cache *regardless of the input*. This implies that eviction can be determined by only inspecting KVs and that an attention-free cache eviction criteria exists. In fact, we observe that *keys with lower average pairwise cosine similarity also have higher attention outputs*, as shown in Figure 2.

Motivated by these observations, we propose an eviction method called KEYDIFF, that evicts keys from the cache with the highest cosine similarity to a cache representative called an *anchor*. We also show that KEYDIFF computes the optimal solution of the KV cache selection problem that minimizes pairwise key cosine similarity. Our experiments demonstrate that KEYDIFF can achieve an accuracy drop of $\leq .04\%$ on LongBench (Bai et al., 2024) with 8K token budget ($\sim 23\%$ KV cache reduction), and can match or outperform state-of-the-art eviction methods, especially when using block prompt processing. Our contributions are as follows:

- We present the empirical observation that low pairwise cosine similarity among keys is correlated with higher attention output.
- We design an eviction policy based on this observation, called KEYDIFF, that enables long context LLM inference with limited memory overhead.
- We show that KEYDIFF computes the optimal solution to a KV cache selection problem that maximizes key diversity measured by pairwise cosine similarity.
- We demonstrate the effectiveness of KEYDIFF on the LongBench task suite, achieving only 1.5% and 0.04% performance gap from the eviction-free baseline, using 6K and 8K cache budgets, respectively.

2. Background

2.1. Transformers

The Transformer architecture (Vaswani, 2017) processes input data using a sequence of transformer blocks. A trans-

former block f takes a sequence $X = (x_1, x_2, \dots, x_T) \in \mathbb{R}^{T \times d}$ as input and applies the causal self-attention operator Attention followed by a feed-forward network FF with optional gating (Shazeer, 2020) to produce the output $X' = (x'_1, x'_2, \dots, x'_T) \in \mathbb{R}^{T \times d}$:

$$X' = f(X) = \text{FF}(\text{Attention}(X)), \quad (1)$$

The causal Attention operator projects each input token x_t with matrices $W_q, W_k, W_v \in \mathbb{R}^{d \times d}$ into key, query, and value matrices ($K = XW_k, Q = XW_Q, V = XW_V$, respectively) then applies the following relation to produce the attention output¹:

$$O^{\text{attn}} = \text{Softmax} \left(\frac{QK^\top}{\sqrt{d}} + M \right) V = AV \quad (2)$$

where $O^{\text{attn}} \in \mathbb{R}^{T \times d}$, and the causal attention mask M is an upper triangular matrix with nonzero values of $-\infty$.

2.2. KV Caching

When the Attention operator processes a new token x_{T+1} , it must also recompute the prior KV states for tokens x_0, \dots, x_T . This can be avoided by storing previously computed KVs in a *KV cache* $\mathcal{C} = (K, V)$ for later reuse and append the new KV corresponding x_{T+1} to the cache. We can apply Equation (2) to an existing KV cache \mathcal{C} as follows:

$$o_{T+1}^{\text{attn}} = \text{Softmax} \left(\frac{q_{T+1}[K \| k_{T+1}]^\top}{\sqrt{d}} + M \right) [V \| v_{T+1}], \quad (3)$$

where $k_{T+1}, q_{T+1}, v_{T+1}$ are the key, query, and value states of x_{T+1} , and $[X \| x_{T+1}]$ represents the concatenation of x_{T+1} to an existing tensor X along the time dimension, M is the causal attention mask accounting for both the KV cache and x_{T+1} .

KV caching dramatically reduces the latency of Attention by only computing $k_{T+1}, q_{T+1}, v_{T+1}$ for each token x_{T+1} and reusing the KVs in \mathcal{C} . However, the size of the KV cache increases linearly with the number of processed tokens and dominates the memory footprint in long-context applications (Yang et al., 2024a).

2.3. KV Cache Eviction Methods

To limit the memory footprint of the KV cache, we fix a *cache budget* N , which is the maximum number of tokens to be stored in the cache. If a new KV is added to the cache and the updated cache size is greater than N , we must evict KVs from the cache until the cache budget is met. The *eviction policy* $\pi_N(\mathcal{C})$ evicts a subset of KVs from \mathcal{C} and

¹The multi-head extension and output projections are omitted for brevity.

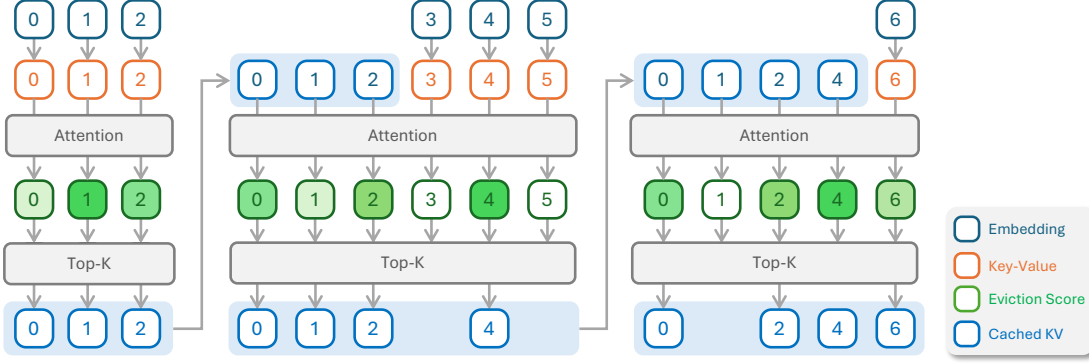


Figure 1: **An example of block prompt processing with KV cache eviction.** The input prompt having length of 7 is segmented by three blocks, and a transformer layer in LLM processes each block by (1) Computing Key-Value states from inputs, (2) computing attention, (3) computing the eviction score, and (4) performing eviction based on the eviction score to satisfy the memory constraints (e.g., at most 4 tokens can reside in the cache). After each block processing, the KV cache is updated and passed to the next round of block processing, satisfying imposed memory constraints on the KV cache.

returns a new cache \mathcal{C}' containing at most N KVs:

$$\begin{aligned} \mathcal{C} &\leftarrow ([K \| k_{t+1}], [V \| v_{t+1}]) \\ \mathcal{C}' &\leftarrow \pi_N(\mathcal{C}) \end{aligned} \quad (4)$$

Attention-Based Eviction Policies Attention-based eviction policies π_N^{attn} use aggregated attention values to rank each KVs' relative importance and keep the N highest scoring KVs. For a given attention weight aggregation function ϕ , the eviction policy π_N^{attn} performs the following steps:

$$\begin{aligned} S &= \text{topk}(\phi(A), N) \\ K' &= \text{gather}(K, S) \\ V' &= \text{gather}(V, S) \end{aligned} \quad (5)$$

where $\text{topk}(x, N)$ returns the indices of N -largest values of x and $\text{gather}(X, S)$ gathers columns indexed by S .

Attention-based eviction methods prioritize KV pairs with higher attention scores to past tokens. This is problematic when applying block prompt processing: all input tokens are not simultaneously accessible within Attention, only those in the current block and cache. This can result in an incorrect eviction decision. Additionally, attention-based eviction often requires explicitly materializing A , which can be resource intensive. We discuss the attention-based eviction policies further in Section 5.

2.4. KV Caching in Resource-Constrained Environments

Existing eviction policies like Zhang et al. (2024b); Oren et al. (2024) focus on processing the entire input prompt *at once*: KVs are computed for each token in the prompt and stored in a cache \mathcal{C} , then the eviction policy π_N is applied to reduce the number of tokens in \mathcal{C}' to N , before token generation. However, the intermediate cache \mathcal{C} before

eviction will grow to the size of the input prompt. This can often exceed model's allocated memory limit when deploying long context applications in resource constrained environments.

As demonstrated in efficient LLM inference frameworks (Agrawal et al., 2023; Holmes et al., 2024; Kwon et al., 2023; Xu et al., 2024a), one solution is to apply π_N more frequently by segmenting X into non-overlapping blocks $X = [X_0, X_1, \dots, X_{m-1}]$, where $X_i = [x_{Bi}, \dots, x_{B(i+1)-1}]$, B is the block size, and $m = \lceil T/B \rceil$, and iteratively updating the cache by exploiting causality, applying Equation (4) in a block-wise fashion:

$$\begin{aligned} \mathcal{C}_i &\leftarrow ([K_{i-1} \| k_{Bi:B(i+1)-1}], [V_{i-1} \| v_{Bi:B(i+1)-1}]) \\ \mathcal{C}'_i &\leftarrow \pi_N(\mathcal{C}_i), \quad \mathcal{C}_i \leftarrow \mathcal{C}'_i, \quad \mathcal{C}_0 = \emptyset, \end{aligned} \quad (6)$$

where $k_{Bi:B(i+1)-1}$ and $v_{Bi:B(i+1)-1}$ are the keys and values selected from X_i respectively, and $\mathcal{C}_i = (K_i, V_i)$ is the KV cache after processing the first i prompt blocks. As in Equation (4), we concatenate the B new KVs to the current cache, apply the eviction policy π_N and update the cache in Equation (6).

We refer to this as *block prompt processing*. Its main advantage is the ability to control of the compute and memory overhead of KV cache management by adjusting the block size B and cache budget N . Note that, in a decoder-based architecture, applying block prompt processing to X with $B = T$ yields the same result as processing all of X at once and choosing $B = 1$ corresponds to the token generation phase of LLM evaluation.

Attention-Based Token Eviction Challenges Despite its advantages, block prompt processing introduces a challenge for KV cache eviction: eviction decisions in block X_i impact the cache used by X_{i+1} , causing eviction errors to compound over time. When the model processes X_i ,

attention-based eviction methods retain KVs with high attention weights derived from X_0, \dots, X_i rather than all of X , which may prematurely evict KVs with high weights in upcoming blocks.

3. Method

We demonstrate a negative correlation between attention scores and the similarity among keys (Section 3.1) and leverage this observation to develop KEYDIFF (Section 3.2), followed by a theoretical justification of the method and preliminary evidence of its efficacy (Section 3.3).

3.1. Correlation of Attention Scores and Key Dissimilarity

To address the shortcomings of attention-based KV cache eviction in Section 2.4, we develop an alternative attention-free scoring metric that retains significant KVs across blocks while being resource efficient. We recall the “attention sink” phenomenon: LLMs often assign high attention weight to the first few tokens, regardless of the input (Xiao et al., 2024; Sun et al., 2024); these highly weighted tokens are called *sink tokens*. However, the index of the sink tokens can vary across heads and layers and reside deeper in the sequence than the first few tokens. This observation motivates the following hypothesis: *high attention scores can be determined by the intrinsic properties of the keys rather than by any particular combination of keys and queries*.

Correlation of Key Similarity and Attention Scores We evaluate our hypothesis by inspecting the cosine similarities between keys computed inside an attention block. We visualize the pairwise cosine similarities between keys along with the attention weights in two particular heads and layers in Figure 2. We observe that keys with lower cosine similarity with other keys exhibit higher relative attention scores regardless of the choice of query, such as the 4th and 15th keys in Figure 2a, or the 1st key in Figure 2b. Pairwise cosine similarity of keys is solely a function of the keys in the cache, which are independent of input queries; the surprising aspect of Figure 2 is the negative correlation with attention weights. These distinctive keys essentially recover the attention sink phenomenon (Xiao et al., 2024).

3.2. KEYDIFF

Based on the observation in Section 3.1, we propose KEYDIFF, which evicts tokens from the KV cache based on key similarity. If the cache \mathcal{C} has intermediate size n and budget N where $n > N$, π_N^{KEYDIFF} is defined as:

$$\begin{aligned} S &= \text{topk}(-\text{CosSim}(K)\mathbf{1}, N) \\ K' &= \text{gather}(K, S) \\ V' &= \text{gather}(V, S) \end{aligned} \quad (7)$$

where $K \in \mathbb{R}^{n \times d}$ and $V \in \mathbb{R}^{n \times d}$ are the cached keys and values, $\text{CosSim}(K) \in \mathbb{R}^{n \times n}$ is the pairwise cosine similarity matrix of keys in K with $\text{CosSim}(K)_{ij} = \frac{\langle k_i, k_j \rangle}{\|k_i\| \|k_j\|}$, and $\mathbf{1} \in \mathbb{R}^n$ is a vector of ones.

Efficient Variant of KEYDIFF Unlike attention-based eviction policies, KEYDIFF does not require access to the attention weights A , facilitating optimized attention kernels that do not materialize A , such as FlashAttention (Dao et al., 2022). However, computing the pairwise cosine similarities runs in $\mathcal{O}(n^2)$ time. Fortunately, the operation

$$\text{topk}(-\text{CosSim}(K)\mathbf{1}, N)$$

can be computed in $\mathcal{O}(n)$ operations on average by computing the score of each token as

$$s_i = -\text{CosSim}(\mu(\hat{K}), \hat{k}_i)$$

where $\mu(\hat{K}) = \frac{1}{n} \sum_{i=1}^n \hat{k}_i$ and $\hat{k}_i = \frac{k_i}{\|k_i\|}$, and retaining the tokens with the N largest scores with a variation of the quick select algorithm. This simplification is derived in Section 3.3.

The eviction score of the efficient expression of KEYDIFF is defined as follows:

$$\begin{aligned} s &= -\text{CosSim}(\mu(\hat{K}), K) \\ S &= \text{topk}(s, N) \end{aligned} \quad (8)$$

We refer to $\mu(\hat{K})$ as the *anchor vector*. Experimentation has shown that the anchor vector $\mu(\hat{K})$ can be replaced with $\mu(K)$ without losing accuracy (see Table 2). We evaluate this efficient version of KEYDIFF described in Figure 3 in the following sections.

3.3. Derivation of KEYDIFF from an Optimization Perspective

To leverage the observation in Section 3.1, we minimize the sum of pairwise cosine similarities of each key retained in the cache. This can be formulated as a constrained optimization problem with the keys $K \in \mathbb{R}^{n \times d}$ whose element is k_i , and budget N smaller than n :

$$\begin{aligned} \underset{S}{\text{minimize}} \quad & \sum_{i \in S} \sum_{j \in S} \frac{k_i \cdot k_j}{\|k_i\| \|k_j\|} \\ \text{subject to} \quad & S \subseteq \{1, \dots, n\}, \\ & |S| = N \end{aligned} \quad (9)$$

This is a combinatorial optimization problem, which is difficult to solve efficiently, particularly during inference. However, we can relax Equation (9) to produce a more tractable approximation to the original problem. First, we rewrite

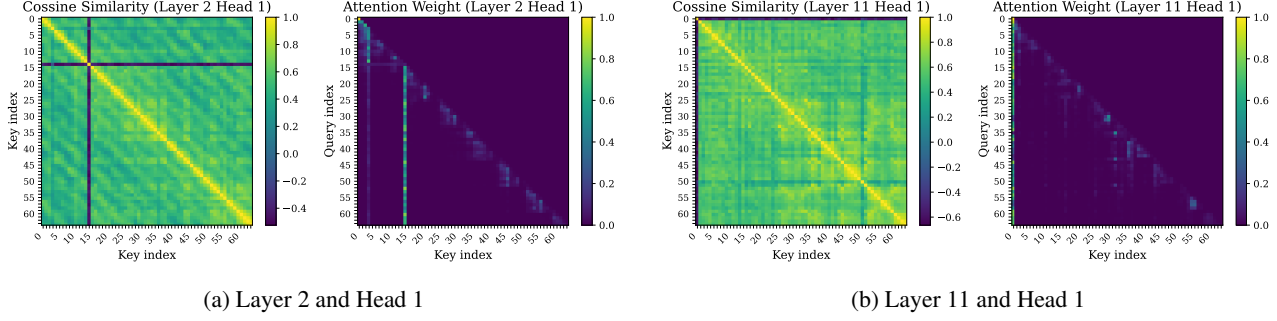


Figure 2: **Cosine similarity of the keys and attention weights.** Measured from Llama 3.2-3B-Instruct and the first sample from the NarrativeQA dataset in LongBench. Truncated to the first 64 tokens for visualization.

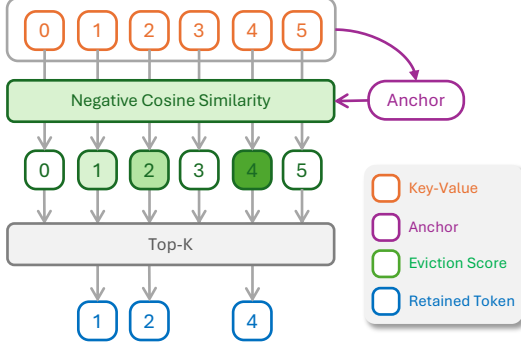


Figure 3: **An overview of KEYDIFF.** (1) KEYDIFF first computes the anchor vector by taking the average of the keys in the KV cache, (2) computes the cosine similarity between the keys and the anchor resulting in eviction scores whose color intensities indicate the score values, and (3) retains the KV pairs with the lowest similarities.

Equation (9) by normalizing keys k_i such that $\hat{k}_i = \frac{k_i}{\|k_i\|}$ resulting in:

$$\sum_{i \in S} \sum_{j \in S} \hat{k}_i \cdot \hat{k}_j = \sum_{i \in S} \hat{k}_i \cdot \left(\sum_{j \in S} \hat{k}_j \right) = \sum_{i \in S} \langle \hat{k}_i, N\mu(\hat{K}_S) \rangle$$

where $\mu(\hat{K}_S) = \frac{1}{N} \sum_{j \in S} \hat{k}_j$ is the empirical mean of normalized keys in S . This objective requires recomputing $\mu(\hat{K}_S)$ for each candidate subset S . The sub-sampled mean tends to converge to the mean over the entire set, the problem can be further relaxed by replacing $\mu(\hat{K}_S)$ with $\mu(\hat{K}) = \frac{1}{n} \sum_{i=1}^n \hat{k}_i$. Dropping N from the objective (since it doesn't affect the solution) yields:

$$\begin{aligned} & \underset{S}{\text{minimize}} \quad \sum_{i \in S} \hat{k}_i \cdot \mu(\hat{K}) \\ & \text{subject to} \quad S \subseteq \{1, \dots, n\}, \\ & \quad |S| = N \end{aligned} \tag{10}$$

The optimal solution of Equation (10) can be found by sorting tokens using their cosine similarity with $\mu(\hat{K})$ and

selecting the smallest N , leading to the algorithm described in Equation (8).

Key Cache Diversity and KEYDIFF To empirically verify KEYDIFF's ability to retain diverse keys, we apply PCA to the keys computed in an attention block of Llama 3.2-3B-Instruct after evaluating a long context prompt. We visualize the distribution of retained and evicted keys by applying sink attention (Xiao et al., 2024), TOVA (Oren et al., 2024), and KEYDIFF as eviction policies in Figure 4. Visual observation reveals the tokens retained by sink attention and TOVA tend to tightly cluster together while KEYDIFF's retained tokens are more evenly distributed. This observation generalizes across heads and layers, as shown in Appendix A.3.

We also visualize the log determinant of the Gram matrix of the key cache $\log(\det(KK^T))$ generated using different eviction policies in Figure 5. This quantity corresponds to the volume of space spanned by the keys in \mathcal{C} . The distribution of volumes for KEYDIFF attains higher values, indicating that the retained keys are more distinctive than TOVA and sink, corroborating the results of Figure 4. Details of how these plots were generated are discussed in Appendix B.1.

4. Experiment

In this section, we empirically demonstrate the effectiveness of KEYDIFF. We begin with a description of competing, state-of-the-art eviction methods, followed by a detailed description of the evaluation setup. We then test each eviction policy on the LongBench task suite (Section 4.2) and report results in Table 1 followed by an ablation study (Section 4.3) of important properties of KEYDIFF. Our findings can be summarized as follows:

- KEYDIFF outperforms competing eviction policies on the Needle-In-A-Haystack benchmark (Kamradt, 2023) (Section 4.1).
- KEYDIFF outperforms competing eviction policies with block size $B = 128$ on LongBench, achieving an 1.5%

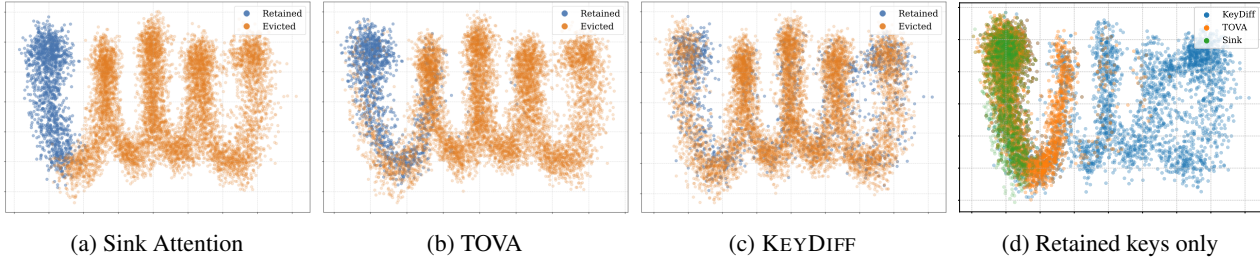


Figure 4: **(a, b, and c)** PCA Visualizations in two dimensions of a key cache managed with Sink, TOVA, and KEYDIFF. Retained tokens are blue, while evicted tokens are orange. The retained tokens using Sink and TOVA cluster together, while KEYDIFF retains more diverse keys. Keys are taken from layer 5 and head 3 of Llama3.2-3B-Instruct, and generated using the NarrativeQA dataset. **(d)** PCA visualization of the retained keys for each KV cache eviction method. We present distributions of additional heads and layers in Appendix A.3.

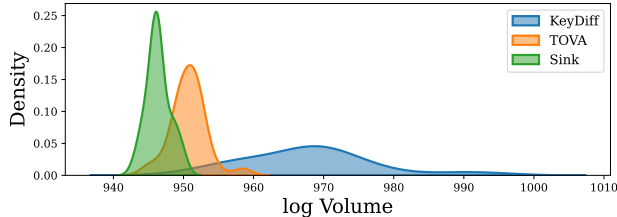


Figure 5: Distribution of $\log(\det(KK^T))$ from the Qasper dataset in LongBench. Larger values mean more of the key space is spanned by the key cache. KEYDIFF retains keys that span a greater volume of the ambient space than TOVA or sink attention.

accuracy drop with a 6K cache budget ($\sim 33\%$ compression rate) and $\leq .04\%$ with a 8k cache budget ($\sim 23\%$ compression rate) with Llama-3.1-8B-Instruct and Llama-3.2-3B-Instruct (Section 4.2).

- KEYDIFF, utilizing negative cosine similarity as the eviction criteria and the mean of cached keys as the anchor vector, generally outperforms other variants of KEYDIFF that use different similarity metrics or anchor vectors. (Section 4.3).

Experimental Setup We apply several cache eviction methods to several decoder-only transformer-based language models, including Llama 3.1-8B-Instruct (Dubey et al., 2024), Llama 3.2-3B-Instruct, and Qwen 2.5-3B/7B-Instruct. We evaluate these models using H2O (Zhang et al., 2024b), TOVA (Oren et al., 2024), SnapKV (Li et al., 2024), and StreamingLLM (Xiao et al., 2024), (or “sink attention”) cache eviction policies, along with the eviction-free model performance as a baseline. We simulate a resource constrained environment by processing prompts and generating responses using Equation (6), with a block size of $B = 128$ for prompt processing and $B = 1$ for token generation using greedy decoding for all experiments. We denote the cache budgets of 2048, 4096, 6144 and 8192 as 2K, 4K, 6K and 8K, respectively.

4.1. Needle In a Haystack

To compare the impact of various cache eviction policies on fact retrieval, we conduct the “Needle In a Haystack” test (Liu et al., 2024a; Kamradt, 2023). This test embeds specific information (“needle”) at different points within a body of unrelated text (“haystack”); finding and retaining the needle is challenging for eviction policies, which can’t know during eviction what information must be retained. The results are shown in Figure 6, where we show the recall accuracy of Llama3.2-3B-Instruct across different document lengths (x-axis) and needle depths (y-axis) with a cache size of 6K. KEYDIFF performs similarly to TOVA and sink attention for shorter documents and outperforms both methods as the document length increases.

4.2. LongBench

LongBench (Bai et al., 2024) is a bilingual, multi-task benchmark suite for LLMs, providing a comprehensive stress test for long prompt inputs. LongBench is useful to evaluate cache eviction methods in a resource constrained environments with a fixed memory budget: 51% of prompts are longer than the largest KV cache size of 8K. For cache budgets of 6k and 8k tokens, prompts in LongBench are compressed by 33% and 23% respectively on average, (see Appendix B.3 for more detail.)

Table 1 summarizes the evaluation results of Llama 3.1-8B-Instruct and Llama 3.2-3B-Instruct on the English subset of LongBench with 2K, 4K, 6K, and 8K cache budgets using various eviction policies with block prompt processing enabled with $B = 128$. We present the full evaluation results in Table 11, and those of Qwen 2.5-3B/7B-Instruct in Table 9.

As shown in Table 1, KEYDIFF outperforms other eviction strategies across most tasks, even demonstrating better performance with smaller cache budgets. KEYDIFF shows significant improvement on the PassageRetrieval-en (PR-en) dataset, which tests whether long-term dependencies within a long prompt can be correctly recognized (Bai et al.,

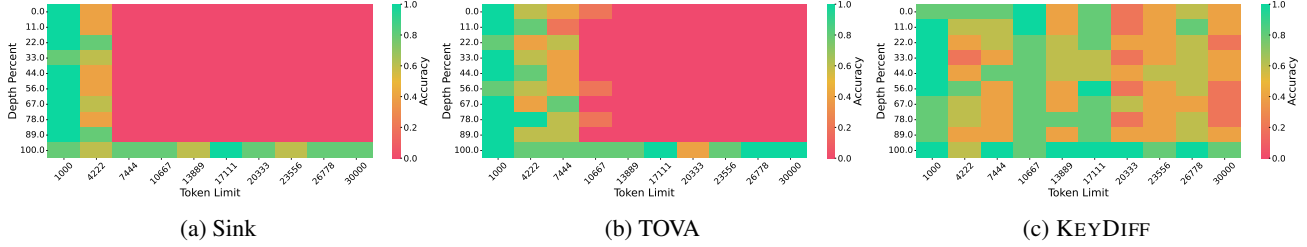


Figure 6: Accuracy across document length and needle depth for needle in a haystack test. Cache size is 6K with $B = 128$.

Table 1: **Llama-3.1-8B/3.2-3B-Instruct LongBench results with $B = 128$ (Higher is better).** We highlight the best and second best methods within a given budget with **bold** and underline. We omit Chinese dataset results and other model results due to space limit. The full evaluation results are in Table 11. \dagger : A subset of samples (183/200) were evaluated due to OOM errors.

		Single Doc. QA			Multi Doc. QA			Summarization			Fewshot Learning			Synthetic		Code		
		Narrative QA	Qasper	MF-en	HotpotQA	2WikiMQA	Musique	GovReport	QMSum	MultiNews	TREC	TriviaQA	SAMSum	PCount	PR-en	Lcc	RB-P	Avg.
Llama3.1-8B		30.05 [†]	47.00	56.12	57.33	47.81	32.25	34.86	25.32	27.02	73.00	91.61	43.37	8.33	99.50	61.66	51.94	49.20
H2O	2K	1.74	21.15	25.33	26.11	24.15	8.78	2.17	2.70	16.78	44.00	29.36	7.62	2.25	5.88	40.15	12.14	16.89
	4K	4.07	36.16	36.00	33.52	32.87	17.78	6.66	5.95	24.09	55.00	47.65	17.41	4.00	24.50	54.85	21.43	26.37
	6K	8.52	43.31	44.80	40.03	42.46	21.68	11.85	8.78	26.03	62.00	56.39	25.72	5.75	45.50	58.62	29.53	33.19
	8K	13.85	44.94	47.81	43.64	44.90	23.65	18.78	11.35	26.49	69.50	69.05	33.41	5.25	62.50	59.74	36.26	38.20
TOVA	2K	22.57	37.26	39.43	45.74	34.48	14.77	28.87	21.17	26.95	62.50	90.73	42.74	0.00	18.00	62.68	52.48	37.52
	4K	22.68	44.55	47.87	46.76	44.54	20.56	30.95	22.13	26.96	61.50	90.56	43.27	3.00	43.50	61.62	53.40	41.49
	6K	24.59	45.93	53.92	55.09	47.43	25.07	32.33	24.10	27.00	68.50	90.81	43.89	4.25	67.00	61.50	52.39	45.24
	8K	24.86	46.78	54.83	54.52	49.00	26.40	33.44	24.76	27.00	71.00	91.11	43.29	6.25	87.00	61.49	51.79	47.09
Sink	2K	21.83	34.27	29.24	38.64	29.50	12.59	28.51	20.21	26.62	65.00	89.46	42.20	2.00	25.50	64.95	59.54	36.88
	4K	22.94	43.01	39.08	44.04	41.39	19.09	31.08	21.57	26.78	70.00	91.53	42.29	3.00	38.50	62.12	58.84	40.95
	6K	25.41	47.40	44.13	47.39	45.73	21.90	32.53	22.19	26.87	72.00	91.25	43.41	3.08	52.50	62.22	56.24	43.39
	8K	23.53	46.63	48.68	49.61	47.16	21.14	33.10	23.20	26.92	72.00	91.29	43.79	3.25	66.00	62.18	56.43	44.68
SnapKV	2K	21.81	37.22	37.19	46.10	35.42	16.53	29.83	21.05	26.77	61.00	88.84	42.56	4.03	51.50	62.37	51.45	39.60
	4K	24.79	44.22	47.30	48.49	46.73	20.55	32.19	22.68	26.95	67.50	90.98	43.14	5.17	89.50	61.44	51.20	45.18
	6K	24.10	45.57	50.44	53.12	48.41	24.27	33.43	23.53	27.03	71.50	92.28	43.58	5.25	98.00	61.32	52.16	47.12
	8K	25.15	46.55	53.39	56.00	48.75	27.82	33.67	24.85	27.01	72.50	91.78	43.54	5.08	100.00	61.48	51.41	48.06
KEYDIFF	2K	26.64	41.73	50.99	51.59	46.47	22.84	29.02	23.86	26.76	66.50	85.92	39.26	3.17	96.00	59.17	39.42	44.33
	4K	28.70	45.62	56.06	54.58	49.31	28.25	32.30	25.03	27.07	70.00	90.85	42.84	4.21	99.00	60.80	48.00	47.66
	6K	29.90	46.33	55.11	56.80	49.50	31.52	33.44	24.58	26.98	72.00	90.99	43.10	5.27	99.50	61.40	49.70	48.51
	8K	33.57	46.77	55.48	56.87	49.37	30.88	34.17	25.12	27.01	72.50	92.28	42.81	5.83	99.50	61.48	50.90	49.03
Llama3.2-3B		23.76	40.23	50.09	50.69	42.29	26.84	33.09	24.30	25.21	72.50	90.11	42.58	3.00	96.50	56.22	56.52	45.87
H2O	2K	1.63	19.96	20.20	18.02	19.56	2.88	0.78	1.55	15.97	41.00	21.97	9.83	0.50	0.50	39.71	13.91	14.25
	4K	2.92	31.94	33.23	24.49	28.08	7.55	5.44	6.30	22.77	53.00	38.85	20.33	1.50	7.50	51.23	22.94	22.38
	6K	4.62	38.81	39.06	34.66	35.52	15.21	10.51	10.01	24.25	61.50	53.23	27.37	0.50	13.00	54.55	32.29	28.44
	8K	9.65	39.66	43.20	38.09	40.41	21.46	17.80	13.28	24.67	70.00	64.30	32.19	2.00	24.50	55.00	39.09	33.46
TOVA	2K	17.14	30.14	32.44	35.96	30.05	13.08	26.15	19.70	25.04	56.50	87.81	40.48	2.50	11.50	55.51	52.36	33.52
	4K	20.52	39.53	42.47	44.12	38.42	18.22	29.36	21.36	24.96	63.50	88.98	41.50	3.00	23.50	55.72	56.66	38.24
	6K	20.22	39.78	45.86	49.08	41.54	20.43	30.50	22.17	25.11	66.50	89.00	42.50	4.00	46.50	55.57	57.53	41.02
	8K	21.08	40.67	49.07	48.69	41.93	23.05	31.64	22.85	25.21	69.00	89.25	42.19	2.50	71.00	55.77	57.47	43.21
Sink	2K	16.85	30.69	26.58	33.26	25.27	13.82	26.74	19.15	25.15	65.00	86.17	40.79	1.50	19.50	56.65	52.73	33.74
	4K	19.46	38.61	36.22	41.97	35.84	13.37	29.34	20.19	25.06	71.00	88.06	41.31	2.50	35.50	56.48	52.43	37.96
	6K	19.33	40.29	37.95	46.48	40.29	15.31	30.43	21.35	25.14	71.50	88.93	42.04	3.50	47.00	56.55	54.11	40.01
	8K	20.15	40.02	41.94	48.15	42.24	16.01	31.64	22.10	25.20	73.00	89.26	42.37	3.50	62.50	56.86	56.63	41.97
SnapKV	2K	17.38	31.37	31.48	37.77	30.05	11.54	27.03	19.93	24.97	59.00	88.13	40.48	3.50	32.50	56.32	55.91	35.46
	4K	19.85	39.22	39.86	46.70	37.98	16.64	29.79	21.21	25.01	65.50	89.35	40.95	2.50	62.50	55.74	56.88	40.60
	6K	20.83	39.65	44.48	49.30	40.18	20.28	31.27	22.73	25.09	69.00	89.95	41.47	4.00	85.00	55.69	57.82	43.55
	8K	20.49	40.80	48.16	47.88	41.65	24.79	31.81	23.46	25.17	70.00	90.17	41.99	5.00	94.00	55.77	57.29	44.96
KEYDIFF	2K	18.29	36.65	45.44	46.09	35.41	13.79	28.16	21.45	25.01	60.00	85.24	37.00	1.00	60.50	54.13	42.01	38.14
	4K	22.34	40.60	49.15	50.14	40.30	21.65	31.38	23.44	25.06	66.50	87.92	41.41	2.50	88.50	55.55	52.24	43.67
	6K	22.29	40.68	50.14	51.74	42.19	24.83	32.39	23.53	25.19	71.00	90.02	42.00	3.00	95.00	55.86	54.39	45.27
	8K	22.41	40.77	50.10	49.83	43.58	28.09	32.78	23.60	25.17	72.00	90.17	42.46	3.50	96.50	55.85	55.65	45.78

2024), while achieving near full-context model performance even with the smallest budget. We observed similar trends in the full LongBench task suite as shown in Table 11.

Results for Full Prompt Processing We also evaluate the methods in more standard inference environments without block prompt processing (i.e., setting the block size of the prompt to $B = \infty$) and summarize the results in Table 7. KEYDIFF exhibits similar or better performance compared to competing methods. Notably, the attention-based methods (e.g., H2O, TOVA, and SnapKV) show significant

performance improvements over the $B = 128$ case. This result supports our hypothesis: an eviction scheme robust to changes in the scope of comparison among tokens is essential in memory constrained environments where token-wise attention weight can't be fully materialized.

4.3. Ablation Study

We evaluate the design choices of KEYDIFF, including the similarity metrics and the choice of the anchor vector, and validate the efficacy of KEYDIFF.

Table 2: **Ablation study results about anchor vector.** Average of Full Longbench results for Llama 3.2-3B-Instruct. KEYDIFF results match Table 11. (Higher is better)

	2K	4K	6K	8K
KEYDIFF	35.09	40.28	41.88	42.40
Pairwise	35.24	40.61	41.87	42.45
Median	35.43	40.67	41.89	42.26

Table 3: **Ablation study results about distance metric.** Average of Full Longbench results of Llama 3.2-3B-Instruct. KEYDIFF results match Table 11. (Higher is better)

	2K	4K	6K	8K
KEYDIFF	35.09	40.28	41.88	42.40
DotProd	30.14	38.01	41.09	42.23
Euclidean	13.68	21.06	25.91	29.53

Selecting the Anchor Vector We have mainly evaluated KEYDIFF using the method described in Equation (8). Scores to determine eviction are measured via cosine similarity with an *anchor vector* which can be computed in several ways. We run LongBench on Llama3.2-3B-Instruct with eviction policies using the following anchor choices: pairwise cosine similarity from Equation (7), denoted Pairwise; KEYDIFF, using the mean of all normalized keys as an anchor, and using the median of keys as an anchor, denoted Median. Table 2 summarizes the average LongBench accuracy for the different methods to Llama 3.2-3B-Instruct. KEYDIFF shows similar average scores to Pairwise. Additionally, KEYDIFF and Median show similar scores, demonstrating that KEYDIFF is robust to the selection of the anchor design.

Selecting the Similarity Metric We use cosine similarity as the scoring metric for eviction in KEYDIFF based on our discussion in Section 2.2. This could be replaced with other metrics like the dot product or Euclidean distance. We evaluate KEYDIFF variants using dot product and Euclidean distance as the similarity metric, denoted DotProd and Euclidean respectively, and report the results in Table 3. KEYDIFF and DotProd show similar performance for 6K and 8K budgets. However, KEYDIFF outperforms DotProd for smaller cache sizes. This implies that considering both the direction and the magnitude of the keys to compute similarity are important for identifying the tokens to evict. On the other hand, Euclidean shows a significant performance drop relative to KEYDIFF.

5. Related Work

Sparse Attention LLMs often exhibit high attention sparsity, where a small subset of keys receives a significant

proportion of attention scores. This characteristic allows sparse approximation techniques to reduce the computational cost of attention. Similar to PagedAttention (Kwon et al., 2023), Tang et al. (2024) estimates the importance of a page (a contiguous set of keys) to a given query, whereas Rehg (2024) further refined the budgets in a per-head manner. On the contrary, sample-based methods (Zhu et al., 2024; Ribar et al.) attempt to approximate token importance by inspecting the attention scores from the last few queries or certain query channel dimensions. Despite their effectiveness in reducing computational costs, these methods do not address the memory overhead of the KV cache, which typically retains all KVs.

KV Cache Compression Different approaches to compress the KV cache include architecture modification such as GQA (Ainslie et al., 2023), which shares a KV cache across a small number of heads. Other techniques to compress the KV cache include quantization such as in (Hooper et al., 2024; Liu et al., 2024b; Zhang et al., 2024a) in which the authors use various techniques to take advantage of existing patterns to efficiently quantize and compress the KV cache. More related to our work (Yang et al., 2024b) uses a scoring mechanism to determine the precision of the quantization for different tokens.

Token Eviction Methods Unlike the sparse attention and KV cache compression methods, eviction methods *evict* KVs from the cache to reduce the size of the KV cache. As discussed in Section 2.3, the majority of the token eviction methods employ their own rules to decide the importance of the tokens by manipulating the attention score A . For example, by appropriately choosing the aggregation functions $\phi(A)$ of Equation (4), we can obtain existing attention-based eviction methods as discussed in Appendix A.1. Attention-based eviction may be a better choice when the entire prompt is being processed at once, as the eviction can be done by assessing the importance of all tokens simultaneously. However, computing the full attention score of long prompts could be prohibitively expensive in resource-constrained environments.

6. Conclusion

Inspired by our observation that distinctive keys tend to have high attention scores, we propose KEYDIFF, a training-free KV cache eviction method based on key similarity that enables large language models to operate in memory and compute constrained environments. We justify KEYDIFF by showing that it computes the optimal solution for an optimization problem minimizing the pairwise cosine similarity among keys in the KV cache. KEYDIFF significantly outperforms state-of-the-art KV cache eviction methods under similar memory constraints, with only a 1.5% and 0.04% ac-

curacy drop from the non-evicting baseline while achieving 33% and 23% KV cache memory reduction on LongBench.

Impact Statement

This paper presents work whose goal is to advance the field of Machine Learning. There are many potential societal consequences of our work, none of which we feel must be specifically highlighted here.

References

Agrawal, A., Panwar, A., Mohan, J., Kwatra, N., Gulavani, B. S., and Ramjee, R. Sarathi: Efficient llm inference by piggybacking decodes with chunked prefills. *arXiv preprint arXiv:2308.16369*, 2023.

Ainslie, J., Lee-Thorp, J., de Jong, M., Zemlyanskiy, Y., Lebrón, F., and Sanghai, S. Gqa: Training generalized multi-query transformer models from multi-head checkpoints. *arXiv preprint arXiv:2305.13245*, 2023.

Alizadeh, K., Mirzadeh, I., Belenko, D., Khatamifard, K., Cho, M., Del Mundo, C. C., Rastegari, M., and Farajtabar, M. Llm in a flash: Efficient large language model inference with limited memory. *arXiv preprint arXiv:2312.11514*, 2023.

Bai, Y., Lv, X., Zhang, J., Lyu, H., Tang, J., Huang, Z., Du, Z., Liu, X., Zeng, A., Hou, L., Dong, Y., Tang, J., and Li, J. LongBench: A bilingual, multitask benchmark for long context understanding. In Ku, L.-W., Martins, A., and Srikumar, V. (eds.), *Proceedings of the 62nd Annual Meeting of the Association for Computational Linguistics (Volume 1: Long Papers)*, pp. 3119–3137, Bangkok, Thailand, August 2024. Association for Computational Linguistics. doi: 10.18653/v1/2024.acl-long.172. URL <https://aclanthology.org/2024.acl-long.172>.

Barbero, F., Arroyo, Á., Gu, X., Perivolaropoulos, C., Bronstein, M., Pascanu, R., et al. Why do llms attend to the first token? *arXiv preprint arXiv:2504.02732*, 2025.

Brown, T., Mann, B., Ryder, N., Subbiah, M., Kaplan, J. D., Dhariwal, P., Neelakantan, A., Shyam, P., Sastry, G., Askell, A., et al. Language models are few-shot learners. *Advances in neural information processing systems*, 33: 1877–1901, 2020.

Dao, T., Fu, D., Ermon, S., Rudra, A., and Ré, C. Flashattention: Fast and memory-efficient exact attention with io-awareness. *Advances in Neural Information Processing Systems*, 35:16344–16359, 2022.

Dubey, A., Jauhri, A., Pandey, A., Kadian, A., Al-Dahle, A., Letman, A., Mathur, A., Schelten, A., Yang, A., Fan, A., et al. The llama 3 herd of models. *arXiv preprint arXiv:2407.21783*, 2024.

Godey, N., de la Clergerie, É., and Sagot, B. Anisotropy is inherent to self-attention in transformers. *arXiv preprint arXiv:2401.12143*, 2024.

Goel, R., Gagrani, M., Jeon, W., Park, J., Lee, M., and Lott, C. Direct alignment of draft model for speculative decoding with chat-fine-tuned llms. *arXiv preprint arXiv:2403.00858*, 2024.

Holmes, C., Tanaka, M., Wyatt, M., Awan, A. A., Rasley, J., Rajbhandari, S., Aminabadi, R. Y., Qin, H., Bakhtiari, A., Kurilenko, L., et al. Deepspeed-fastgen: High-throughput text generation for llms via mii and deepspeed-inference. *arXiv preprint arXiv:2401.08671*, 2024.

Hooper, C., Kim, S., Mohammadzadeh, H., Mahoney, M. W., Shao, Y. S., Keutzer, K., and Gholami, A. Kvquant: Towards 10 million context length llm inference with kv cache quantization. *arXiv preprint arXiv:2401.18079*, 2024.

Kamradt, G. Needle in a haystack - pressure testing llms. GitHub repository, 2023. URL https://github.com/gkamradt/LLMTest_NeedleInAHaystack.

Kojima, T., Gu, S. S., Reid, M., Matsuo, Y., and Iwasawa, Y. Large language models are zero-shot reasoners. *Advances in neural information processing systems*, 35: 22199–22213, 2022.

Kwon, W., Li, Z., Zhuang, S., Sheng, Y., Zheng, L., Yu, C. H., Gonzalez, J., Zhang, H., and Stoica, I. Efficient memory management for large language model serving with pagedattention. In *Proceedings of the 29th Symposium on Operating Systems Principles*, pp. 611–626, 2023.

Lewis, P., Perez, E., Piktus, A., Petroni, F., Karpukhin, V., Goyal, N., Kütller, H., Lewis, M., Yih, W.-t., Rocktäschel, T., et al. Retrieval-augmented generation for knowledge-intensive nlp tasks. *Advances in Neural Information Processing Systems*, 33:9459–9474, 2020.

Li, Y., Huang, Y., Yang, B., Venkitesh, B., Locatelli, A., Ye, H., Cai, T., Lewis, P., and Chen, D. Snapkv: Llm knows what you are looking for before generation. *arXiv preprint arXiv:2404.14469*, 2024.

Liu, N. F., Lin, K., Hewitt, J., Paranjape, A., Bevilacqua, M., Petroni, F., and Liang, P. Lost in the middle: How language models use long contexts. *Transactions of the Association for Computational Linguistics*, 12:157–173, 2024a.

Liu, Z., Yuan, J., Jin, H., Zhong, S., Xu, Z., Braverman, V., Chen, B., and Hu, X. Kivi: A tuning-free asymmetric 2bit quantization for kv cache. *arXiv preprint arXiv:2402.02750*, 2024b.

Liu, Z., Zhao, C., Iandola, F., Lai, C., Tian, Y., Fedorov, I., Xiong, Y., Chang, E., Shi, Y., Krishnamoorthi, R., et al. Mobilellm: Optimizing sub-billion parameter language models for on-device use cases. *arXiv preprint arXiv:2402.14905*, 2024c.

Oren, M., Hassid, M., Adi, Y., and Schwartz, R. Transformers are multi-state rnns. *arXiv preprint arXiv:2401.06104*, 2024.

Raffel, C., Shazeer, N., Roberts, A., Lee, K., Narang, S., Matena, M., Zhou, Y., Li, W., and Liu, P. J. Exploring the limits of transfer learning with a unified text-to-text transformer. *Journal of machine learning research*, 21 (140):1–67, 2020.

Rehg, I. Kv-compress: Paged kv-cache compression with variable compression rates per attention head. *arXiv preprint arXiv:2410.00161*, 2024.

Ribar, L., Chelombiev, I., Hudlass-Galley, L., Blake, C., Luschi, C., and Orr, D. Sparq attention: Bandwidth-efficient llm inference. In *Forty-first International Conference on Machine Learning*.

Shazeer, N. Glu variants improve transformer. *arXiv preprint arXiv:2002.05202*, 2020.

Sun, M., Chen, X., Kolter, J. Z., and Liu, Z. Massive activations in large language models. *arXiv preprint arXiv:2402.17762*, 2024.

Tang, J., Zhao, Y., Zhu, K., Xiao, G., Kasikci, B., and Han, S. Quest: Query-aware sparsity for efficient long-context llm inference. *arXiv preprint arXiv:2406.10774*, 2024.

Touvron, H., Martin, L., Stone, K., Albert, P., Almahairi, A., Babaei, Y., Bashlykov, N., Batra, S., Bhargava, P., Bhosale, S., et al. Llama 2: Open foundation and fine-tuned chat models. *arXiv preprint arXiv:2307.09288*, 2023.

van Baalen, M., Kuzmin, A., Nagel, M., Couperus, P., Bastoul, C., Mahurin, E., Blankevoort, T., and Whatmough, P. Gptvq: The blessing of dimensionality for llm quantization. *arXiv preprint arXiv:2402.15319*, 2024.

Vaswani, A. Attention is all you need. *Advances in Neural Information Processing Systems*, 2017.

Wei, J., Wang, X., Schuurmans, D., Bosma, M., Xia, F., Chi, E., Le, Q. V., Zhou, D., et al. Chain-of-thought prompting elicits reasoning in large language models. *Advances in neural information processing systems*, 35:24824–24837, 2022.

Xiao, G., Tian, Y., Chen, B., Han, S., and Lewis, M. Efficient streaming language models with attention sinks. In *The Twelfth International Conference on Learning Representations*, 2024.

Xu, D., Zhang, H., Yang, L., Liu, R., Huang, G., Xu, M., and Liu, X. Empowering 1000 tokens/second on-device llm prefilling with mllm-npu. *arXiv preprint arXiv:2407.05858*, 2024a.

Xu, Y., Jie, Z., Dong, H., Wang, L., Lu, X., Zhou, A., Saha, A., Xiong, C., and Sahoo, D. Think: Thinner key cache by query-driven pruning. *arXiv preprint arXiv:2407.21018*, 2024b.

Yang, D., Han, X., Gao, Y., Hu, Y., Zhang, S., and Zhao, H. Pyramidinfer: Pyramid kv cache compression for high-throughput llm inference. *arXiv preprint arXiv:2405.12532*, 2024a.

Yang, J. Y., Kim, B., Bae, J., Kwon, B., Park, G., Yang, E., Kwon, S. J., and Lee, D. No token left behind: Reliable kv cache compression via importance-aware mixed precision quantization. *arXiv preprint arXiv:2402.18096*, 2024b.

Yao, S., Yu, D., Zhao, J., Shafran, I., Griffiths, T., Cao, Y., and Narasimhan, K. Tree of thoughts: Deliberate problem solving with large language models. *Advances in Neural Information Processing Systems*, 36, 2024.

Zhang, T., Yi, J., Xu, Z., and Shrivastava, A. Kv cache is 1 bit per channel: Efficient large language model inference with coupled quantization. *arXiv preprint arXiv:2405.03917*, 2024a.

Zhang, Z., Sheng, Y., Zhou, T., Chen, T., Zheng, L., Cai, R., Song, Z., Tian, Y., Ré, C., Barrett, C., et al. H2o: Heavy-hitter oracle for efficient generative inference of large language models. *Advances in Neural Information Processing Systems*, 36, 2024b.

Zhu, Q., Duan, J., Chen, C., Liu, S., Li, X., Feng, G., Lv, X., Cao, H., Chuanfu, X., Zhang, X., et al. Sampleattention: Near-lossless acceleration of long context llm inference with adaptive structured sparse attention. *CoRR*, 2024.

KEYDIFF

Supplementary Material

A. Extended Related Work

A.1. Attention-based eviction methods

In this section, we provide a unified framework to understand prominent attention-based eviction methods. As mentioned in Equation (5), we can specify attention-based eviction methods under the unified framework with proper selection of the aggregation function $\phi(A)$ as follows:

- TOVA (Oren et al., 2024): $\phi^{\text{TOVA}}(A) = A_{-1,:}$,
- H2O (Zhang et al., 2024b): $\phi^{\text{H2O}}(A) = A_{\text{prev}} + A^\top 1$,
- SnapKV (Xiao et al., 2024): $\phi^{\text{SnapKV}}(A) = (A^\top 1) * K$, where K is a vector of $\frac{1}{k}$ and k is the kernel size of average smoothing.

A.2. Runtime and Memory Complexity

We analyze the runtime and memory complexity for the prominent KV cache eviction algorithms in Table 4. For a given block size B and cache budget N , KEYDIFF requires $\mathcal{O}(N + B)$ runtime and memory. The same holds true for TOVA, since it only requires computing the bottom row of A . Sink attention retains the k first tokens in the input sequence, followed by a sliding window of size L , resulting in $\mathcal{O}(k + L) = \mathcal{O}(N)$ memory and runtime, since $k + L$ equals the chosen cache budget. SnapKV computes attention over a sliding window of size L against $N + B$ keys from the incoming block and the key cache, so the memory and runtime complexity is $\mathcal{O}((N + B)L)$. H2O accumulates attention weights over all tokens, and computes the attention over the current block, so it will require $\mathcal{O}(NB + B^2)$ memory overhead and runtime. We summarize these details in Table 4

Table 4: **Runtime and memory complexity of token eviction methods.**

	Runtime Complexity	Memory Complexity
KEYDIFF	$\mathcal{O}(N + B)$	$\mathcal{O}(N + B)$
TOVA	$\mathcal{O}(N + B)$	$\mathcal{O}(N + B)$
H2O	$\mathcal{O}(NB + B^2)$	$\mathcal{O}(NB + B^2)$
SnapKV	$\mathcal{O}((N + B)L)$	$\mathcal{O}((N + B)L)$
Sink	$\mathcal{O}(N)$	$\mathcal{O}(1)$

A.2.1. FLOP COUNT OF KEYDIFF

Regarding the FLOP count of KeyDiff: the bulk of the computation in KeyDiff (neglecting the ‘topk’ operator) is the following two expressions:

- $\mu(\hat{K}) = \frac{1}{n} \sum_{i=1}^n \frac{k_i}{\|k_i\|}$
- $s_i = \text{CosSim}(\mu(\hat{K}), k_i) = \frac{\mu(\hat{K}) \cdot k_i}{\max(\|\mu(\hat{K})\| \cdot \|k_i\|, \epsilon)}, \quad i = 1, \dots, n$

We will count the total number of additions, multiplications, square roots and divisions required by KeyDiff separately, since division and square root implementation are hardware-dependent, then assign weights to each operation at the end for a final count. Norms are assumed to be 2-norms. We count the FLOPs required for each operation as follows:

- $\|k_i\| = \sqrt{k_i \cdot k_i}$: since $k_i \in \mathbb{R}^d$: d multiplications, $d - 1$ additions, one square root. Repeating for each i , this contributes nd multiplications, $n(d - 1)$ additions, and n square roots.
- $\frac{k_i}{c}$: naively, d divisions, but can be rewritten as one division and d multiplications. Repeating for each i , this contributes nd multiplications and n divisions.
- $\frac{1}{n} \sum_{i=1}^n c_i$, for $c \in \mathbb{R}^d$: one division, $(n - 1)d$ additions.

Combining the above, we can compute the anchor vector using $2nd$ multiplications, $2nd - n - d$ additions, n square roots and $n + 1$ divisions.

To compute the cosine similarity score, we have from above that $\mu(\hat{K}) \cdot k_i$ requires nd multiplications and $n(d - 1)$ additions. Also from above, we have that computing $\|\mu(\hat{K})\|$ requires d multiplications, $d - 1$ additions and one square root. We reuse the computation of $\|k_i\|$ from the previous step and compute $\|k_i\| \|\mu(\hat{K})\|$ in n multiplications and $\max(\|k_i\| \|\mu(\hat{K})\|, \epsilon)$ with more n additions (assuming boolean comparison is equals addition in cost). We can then divide through to compute $\frac{\mu(\hat{K}) \cdot k_i}{\max(\|k_i\| \|\mu(\hat{K})\|, \epsilon)}$ with n divisions. Therefore, computing the cosine similarity between the anchor and each key requires $nd + d + n$ multiplications, $nd + d - 1$ additions, $n + 1$ divisions and one square root.

Adding everything up, KeyDiff requires:

1. $3nd + d + n$ multiplications,
2. $3nd - n - 1$ additions,
3. $2n + 2$ divisions,
4. $n + 1$ square roots,

If we declare additions and multiplications are roughly one FLOP (i.e. can be computed in one cycle), division is roughly 5 FLOPs and square root is roughly 8 FLOPs, we arrive at a final FLOP count of:

$$(3nd + d + n) + (3nd - n - 1) + 5 * (2n + 2) + 8 * (n + 1) = (6d + 18)n + d + 17. \quad (\text{A.1})$$

This is linear in the number of keys n with a small constant, relative to the quadratic complexity of the attention operator.

A.3. Additional PCA Visualizations

In order to demonstrate the phenomena in Figure 4 persists across all heads and layers, we have included several more visualizations as seen in Figure 7, Figure 8, and Figure 9.

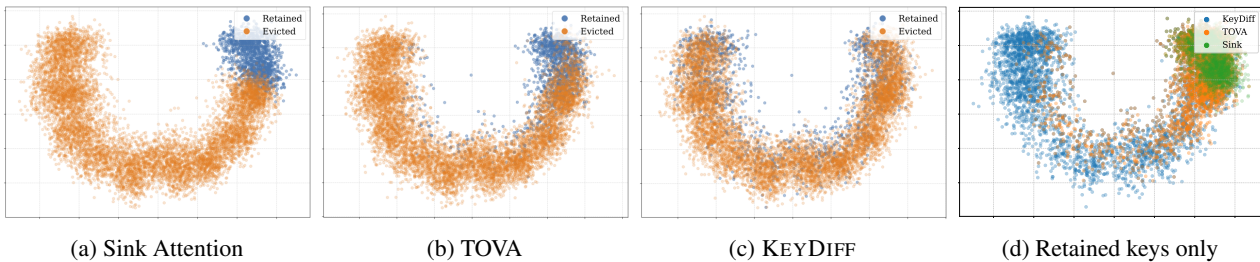
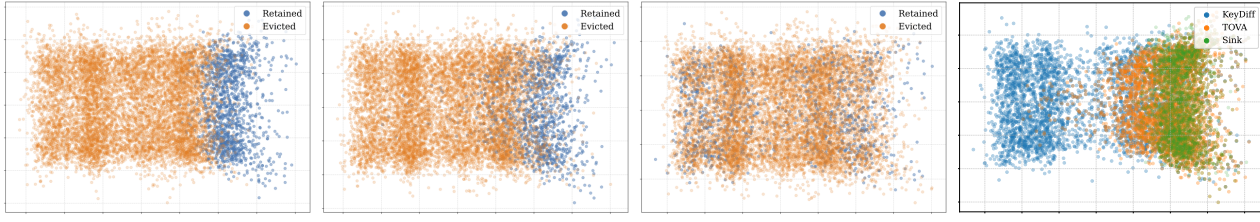


Figure 7: **(a, b, and c)** PCA Visualizations in two dimensions of a key cache managed with Sink, TOVA, and KEYDIFF. Retained tokens are blue, while evicted tokens are orange. Keys are taken from layer 27 and head 4 of Llama3.2-3B-Instruct, and generated using the NarrativeQA dataset. **(d)** PCA visualization of the retained keys for each KV cache eviction method



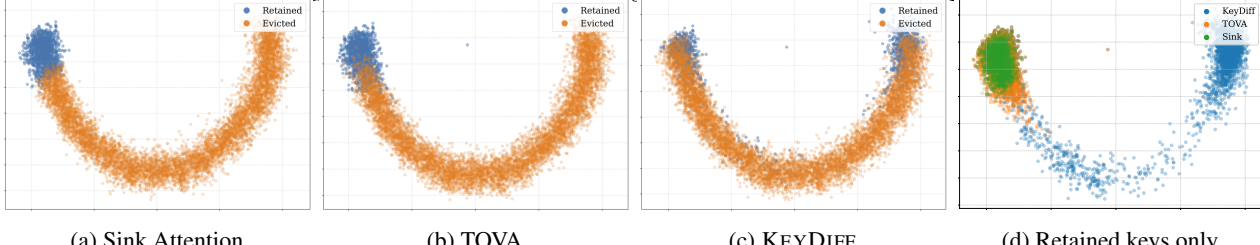
(a) Sink Attention

(b) TOVA

(c) KEYDIFF

(d) Retained keys only

Figure 8: Keys taken from layer 20 and head 0 of Llama3.2-3B-Instruct



(a) Sink Attention

(b) TOVA

(c) KEYDIFF

(d) Retained keys only

Figure 9: Keys taken from layer 8 and head 1 of Llama3.2-3B-Instruct

B. Additional discussion for LongBench

B.1. Empirical Motivation for KEYDIFF Setup

To generate Figure 4, we used the first sample from the test split of the narrativeqa task in LongBench to prefill the KV cache of Llama3.2-3B-Instruct with a block size of $B = 128$. The KV cache had a maximum size of 4096 while the sample was much longer, requiring KV eviction. We applied PCA to the key cache and repeated the process for sink attention, TOVA and KEYDIFF.

To construct Figure 5, we sample 100 prompts from the Qasper dataset in LongBench (Bai et al., 2024), compute the log determinant of KK^T of the keys in the KV caches of each head and layer of Llama 3.2-3B-Instruct using a cache budget of $N = 2048$ and a block size of $B = 128$, and plot the distribution in Figure 5. We show this key distribution for sink attention, TOVA and KEYDIFF.

B.2. Experiment Setup

In this subsection, we provide the experimental setup for KEYDIFF and the baselines for the LongBench experiments. The LongBench evaluation is conducted using the default parameters of the LongBench evaluator with predefined prompt templates. The prompt block size is set to $B = 128$, and the same B value is used for all experiments.

For TOVA, H2O, and SnapKV, the set of attention weights computed from a single key cache due to grouped query attention (Ainslie et al., 2023) is aggregated by taking the average over the attention weights. Additionally, only for SnapKV, we apply average smoothing to the attention score with a kernel size of 7 and keep the most recent 32 tokens in the cache, following the suggestion of the original paper. For Sink, we used the first four tokens as the attention sink, following the suggestion of the original paper.

B.3. Longbench dataset statistics

In this section, we provide the length statistics of the Longbench Benchmark and in-depth analysis of compression ratios for the given KV cache budgets, such as 2K, 4K, 6K, and 8K.

Prompt lengths We measure the number of tokens in the samples using LLama tokenizer (Touvron et al., 2023). As shown in Figure 10, LongBench exhibits variability in sample length from the datasets.

Compression ratio The majority of other KV cache eviction studies assume an unconstrained memory footprint. Before they compress the cache by applying an eviction policy, they first set the target compression ratio and evict the appropriate number of KV pairs to satisfy the compression ratio (Zhang et al., 2024b; Oren et al., 2024; Li et al., 2024). On the other hand, we fix the KV cache size and ensure the number of cached tokens is less than or equal to the predefined cache size.

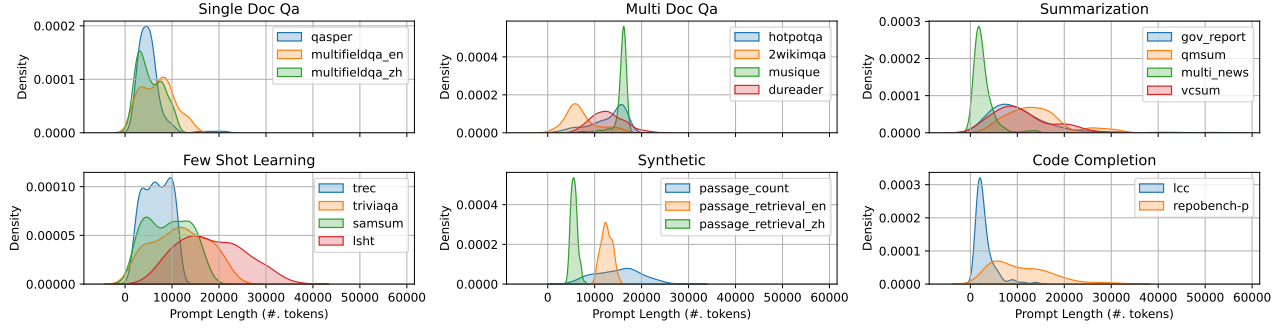


Figure 10: Histograms of sample lengths measured by number of tokens

Due to these differences, it is less straightforward to set appropriate KV cache budgets to satisfy the target compression ratios. Instead, we provide the average compression ratio, which is defined as:

$$\text{Average Compression Ratio} = \frac{1}{I} \sum_{i=1}^I \frac{N}{L_i},$$

where N is the KV cache budget, and L_i is the length of the i -th prompt (sample). We replace the summand with 1 whenever $N \geq L_i$, as compression doesn't occur in that setting.

As summarized in Table 6, 2K cache budgets have a 0.31 average compression ratio, which indicates 69% of input prompts are compressed. Our largest cache budget, 8K, exhibits a 0.77 average compression ratio.

	$\leq 2K$	$2K \leq L \leq 4K$	$4K \leq L \leq 6K$	$6K \leq L \leq 8K$	$\geq 8K$	Total
NarrativeQA	0	0	0	8	192	200
Qasper	1	77	83	25	14	200
MultifidelityQA-En	9	31	21	32	57	150
MultifidelityQA-Zh	14	69	47	33	37	200
HotPotQA	1	4	12	12	171	200
2wikimqa	8	17	68	54	53	200
musique	0	0	0	3	197	200
dureader	0	0	0	16	184	200
gov report	0	20	29	45	106	200
qmsum	0	1	17	15	167	200
multi news	99	71	19	6	5	200
vcsum	4	20	18	32	126	200
trec	4	43	41	39	73	200
triviaqa	4	21	15	21	139	200
samsun	6	29	34	17	114	200
lsht	0	0	3	8	189	200
passage count	0	0	3	13	184	200
passage-retrieval-En	0	0	0	0	200	200
passage-retrieval-Zh	0	0	160	10	0	170
lcc	80	86	21	4	9	200
repobench-p	0	25	37	25	113	200

Table 5: Distribution of sample length measured by Llama2 tokenizer

B.4. Additional Results

C. Attention Sinks and Approximate Collinearity

To better understand why there exists a negative correlation between cosine similarity between keys and attention scores, we look to recent research that seeks to the importance of attention sinks in decoder-based LLMs. The authors in (Barbero et al.,

	2K	4K	6K	8K
NarrativeQA	0.10	0.20	0.30	0.40
Qasper	0.47	0.82	0.96	0.98
MultifidelityQA-En	0.40	0.66	0.82	0.93
MultifidelityQA-Zh	0.49	0.78	0.91	0.98
HotPotQA	0.19	0.37	0.52	0.66
2wikimqa	0.36	0.65	0.85	0.92
musique	0.13	0.27	0.40	0.53
dureader	0.17	0.34	0.52	0.68
gov report	0.28	0.52	0.70	0.81
qmsum	0.18	0.36	0.52	0.66
multi news	0.81	0.96	0.98	0.53
vcsum	0.27	0.49	0.65	0.68
trec	0.38	0.66	0.84	0.94
triviaqa	0.26	0.46	0.60	0.72
samsun	0.32	0.55	0.71	0.82
lsht	0.13	0.27	0.39	0.52
passage count	0.15	0.31	0.46	0.60
passage-retrieval-En	0.16	0.33	0.49	0.66
passage-retrieval-Zh	0.37	0.74	0.99	1.00
lcc	0.78	0.95	0.98	0.99
repobench-p	0.27	0.52	0.67	0.78
average	0.31	0.53	0.67	0.77

Table 6: Compression ratio of prompts w.r.t. various KV cache budgets

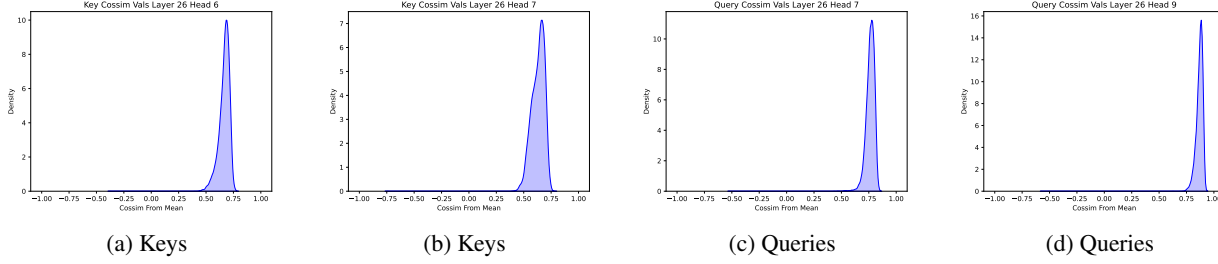


Figure 11: Angular distributions of keys and queries measured with respect to mean key and mean query

2025) show that attention sinks emerge from training decoder-based LLMs since they can denoise the model and prevent rank collapse by limiting over mixing in attention heads. Moreover, attention patterns in decoder based models demonstrate that most attention logits are quite small (and almost always negative) for most keys and queries. This allows the attention sink to have high attention activation, preventing over mixing in addition to allowing the heads to specialize and selectively identify important tokens.

At the same time, the results in (Godey et al., 2024) suggest that hidden states, keys and queries are all approximately collinear in the sense that $\text{CosSim}(x_i, x_j) \gg 0$. In geometric terms, this means that most key tokens and query tokens lie in the same direction in Euclidean space. Our own results, seen in Figure 11 demonstrate that this is the case for both keys and queries. Our experiments show that most keys and queries lie within a small angular distance from the mean key and query. More than this, we see that across all heads, the mean key and mean query have negative cosine similarity Figure 12. Moreover, as seen in Figure 13, we find that the norms of keys and queries are tightly clustered around a relatively fixed value. This means that variations in the norm of key and query tokens have less impact on the magnitude of attention scores than their direction. These three observations indicate that most keys and queries combine to create uniformly small attention logits, and that larger attention weights are constructed by projecting keys closer to the direction of the mean query. This appears to be the fundamental mechanism through which over mixing is prevented: if most attention activations are very small, each head can increase the activations of a small number of keys across most queries selectively projecting them to be more aligned with the distribution of queries. This hypothesis is further supported by the fact that sink tokens

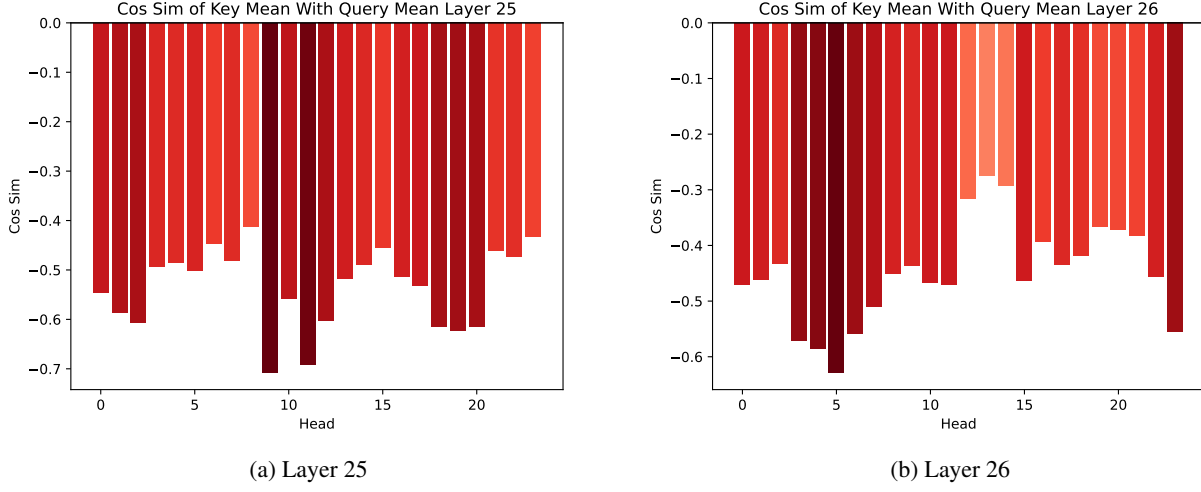


Figure 12: Cosine Similarity of mean key and mean query for each head in several layers.

themselves often have small norm, which results in an approximate no-op in the attention head as in (Barbero et al., 2025), however in this case, the only way for a key corresponding to a sink token to have high attention scores is if it is as parallel as possible to the set of query tokens.

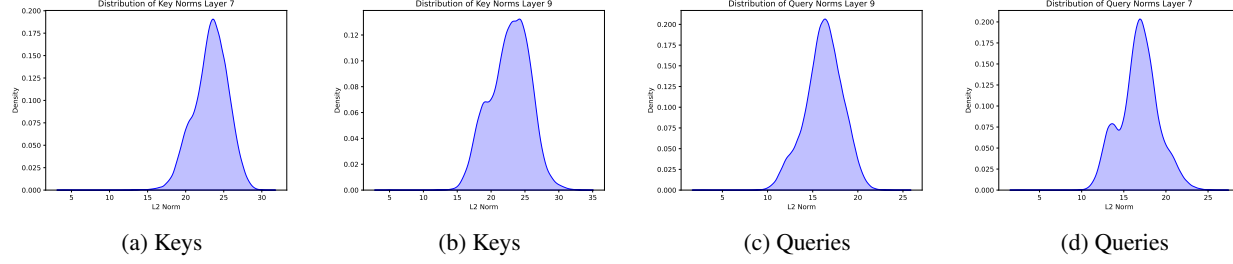


Figure 13: Distribution of L2 norms for keys and queries in several layers.

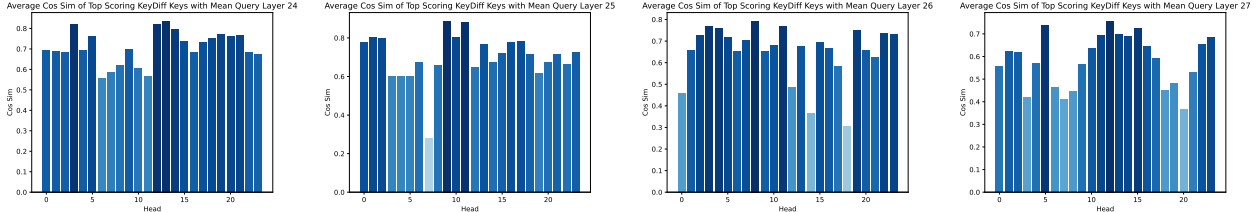


Figure 14: Average cosine similarity per head between high scoring keydiff key tokens and mean query.

To verify the above hypothesis, we show Figure 14 that keys which have maximum angular difference from the mean key are aligned with the mean query, resulting in very large attention weights. This demonstrates how LLMs exploit the geometry of the hidden states and projections to limit over mixing, and selectively identify important tokens.

To summarize, we have for all attention heads in decoder based transformer models:

- The majority of keys and queries are approximately collinear with their mean.
- Mean keys and mean queries have negative cosine similarity across all heads.
- Most keys and queries have a similar L2 norm.
- Decoder based attention heads can selectively increase attention weights for a fixed key by aligning it with the mean query.
- Key token importance can hence be measured by the angular distance between a key and the mean key.

We can show mathematically with some reasonable assumptions based on the above observations that key tokens with persistently high attention scores must be geometrically aligned with queries.

Theorem C.1. Suppose that for a fixed query token q , there is a set of key tokens $\{k_i\}_{i=1}^n$ such that $\|k_i\|_2^2 < M$, $\forall i$. Without loss of generality suppose $\|q\| = 1$ and assume k^* is a key not in $\{k_i\}_{i=1}^n$ with $\|k^*\|_2^2 < M$ that has attention weight $w > 0$:

$$w = \frac{\exp(k^{*\top} q)}{\exp(k^{*\top} q) + \sum_{i=1}^n \exp(k_i^\top q)}.$$

Then

$$\frac{\log(\frac{n}{n+1}) - \log(1-w)}{2M} - 1 \leq \text{CosSim}(k^*, q)$$

Proof. To show this we have that

$$\begin{aligned} w &= \frac{\exp(k^{*\top} q)}{\exp(k^{*\top} q) + \sum_{i=1}^n \exp(k_i^\top q)} \\ w \left(\exp(k^{*\top} q) + \sum_{i=1}^n \exp(k_i^\top q) \right) &= \exp(k^{*\top} q) \\ w \sum_{i=1}^n \exp(k_i^\top q) &= (1-w) \exp(k^{*\top} q) \end{aligned}$$

Note that $-M \leq k_i^\top q \leq M$ and hence

$$\begin{aligned} w \sum_{i=1}^n \exp(-M) &\leq (1-w) \exp(k^{*\top} q) \\ wn \exp(-M) &\leq (1-w) \exp(k^{*\top} q) \\ \frac{wn \exp(-M)}{1-w} &\leq \exp(k^{*\top} q) \\ \log(wn) - M - \log(1-w) &\leq M \text{CosSim}(k^*, q) \\ \frac{\log(wn) - M - \log(1-w)}{M} &\leq \text{CosSim}(k^*, q) \\ \frac{\log\left(\frac{\exp(k^{*\top} q)}{\exp(k^{*\top} q) + \sum_{i=1}^n \exp(k_i^\top q)} n\right) - M - \log(1-w)}{M} &\leq \text{CosSim}(k^*, q) \\ \frac{\log\left(\frac{\exp(k^{*\top} q)}{(n+1) \exp(M)} n\right) - M - \log(1-w)}{M} &\leq \text{CosSim}(k^*, q) \\ \frac{-M \text{CosSim}(k^*, q) + \log(\frac{n}{n+1}) - 2M - \log(1-w)}{M} &\leq \text{CosSim}(k^*, q) \\ \frac{\log(\frac{n}{n+1}) - 2M - \log(1-w)}{M} &\leq 2 \text{CosSim}(k^*, q) \\ \frac{\log(\frac{n}{n+1}) - \log(1-w)}{2M} - 1 &\leq \text{CosSim}(k^*, q) \end{aligned}$$

□

The above proof demonstrates that as long as the norms of the keys are bounded, in order for an attention head to be able to freely allocate w attention weight to a given key k^* , the cosine similarity between k^* and q must be high, therefore k^* and q must be approximately collinear.

Using this result, we can also show that as long as the cosine similarity between k^* and q is high, while the cosine similarity between \bar{k} and q is low, $\text{CosSim}(k^*, \bar{k})$ is small. Note that, since empirical results demonstrate that most keys have high cosine similarity with their mean \bar{k} , a key with high importance, approximately collinear to q , will also have low cosine similarity to \bar{k} . Generally, this also suggests that key tokens with low cosine similarity to \bar{k} have greater importance.

In order to show this, we need the following auxiliary result.

Lemma C.2. *Suppose $\{x_1, \dots, x_n\}$ is an orthonormal basis of \mathbb{R}^n and $y \in \mathbb{R}^n$. Define $\alpha_i = \text{CosSim}(x_i, y)$. Then $\sum_{i=1}^n \alpha_i^2 = 1$.*

Proof. Note that $\alpha_i = \frac{y^\top x_i}{\|y\| \|x_i\|} = \frac{y^\top x_i}{\|y\|}$. If we expand $\frac{y}{\|y\|}$ in the basis $\{x_1, \dots, x_n\}$ we see that

$$\begin{aligned} \frac{y}{\|y\|} &= \sum_{i=1}^n \left(\frac{y}{\|y\|}^\top x_i \right) x_i \\ &= \sum_{i=1}^n \alpha_i x_i \end{aligned}$$

But then, we know that since $\left\| \frac{y}{\|y\|} \right\|_2^2 = 1$, then $\left\langle \sum_{i=1}^n \alpha_i x_i, \sum_{i=1}^n \alpha_i x_i \right\rangle = 1$. But we have

$$\begin{aligned} \left\langle \sum_{i=1}^n \alpha_i x_i, \sum_{i=1}^n \alpha_i x_i \right\rangle &= \sum_{i=1}^n \sum_{j=1}^n \langle \alpha_i x_i, \alpha_j x_j \rangle \\ &= \sum_{i=1}^n \langle \alpha_i x_i, \alpha_i x_i \rangle \\ &= \sum_{i=1}^n \alpha_i^2 \end{aligned}$$

proving the result. \square

Theorem C.3. *Consider tokens k^* , q , \bar{k} as above where \bar{k} is the average of the keys tokens. Suppose $\text{CosSim}(k^*, q) = \beta_q > 0$ and $\text{CosSim}(\bar{k}, q) = \alpha_q < 0$. Then $\text{CosSim}(\bar{k}, k^*) \leq 1 + \alpha_q \beta_q - \frac{1}{2} \alpha_q^2 - \frac{1}{2} \beta_q^2$.*

Proof. Consider the cosine similarity of \bar{k} and k^* :

$$\text{CosSim}(\bar{k}, k^*) = \frac{k^{*\top} \bar{k}}{\|k^*\| \|\bar{k}\|}$$

expand \bar{k} in an orthonormal basis which contains $q, \{q, r_1, \dots, r_{n-1}\}$ such that

$$\bar{k} = \|\bar{k}\| \left(\alpha_q q + \sum_{i=1}^{n-1} \alpha_i r_i \right)$$

where $\alpha_i = \text{CosSim}(\bar{k}, r_i)$. Additionally, define $\beta_i = \text{CosSim}(k^*, r_i)$ and note that by the definition of an orthonormal basis and the cosine similarity operation, using the result from [Lemma C.2](#) we have that $\alpha_q^2 + \sum_{i=1}^{n-1} \alpha_i^2 = 1$ and that $\beta_q^2 + \sum_{i=1}^{n-1} \beta_i^2 = 1$. Now we have that

$$\begin{aligned}
 \frac{k^{*\top} \bar{k}}{\|k^*\| \|\bar{k}\|} &= \frac{k^{*\top} \left(\|\bar{k}\| \alpha_q q + \sum_{i=1}^{n-1} \|\bar{k}\| \alpha_i r_i \right)}{\|k^*\| \|\bar{k}\|} \\
 &= \alpha_q \beta_q + \frac{1}{\|k^*\|} \sum_{i=1}^{n-1} \alpha_i k^{*\top} r_i \\
 &= \alpha_q \beta_q + \sum_{i=1}^{n-1} \alpha_i \beta_i \\
 &\leq \alpha_q \beta_q + \sum_{i=1}^{n-1} |\alpha_i| |\beta_i|
 \end{aligned}$$

Applying Young's inequality we obtain

$$\begin{aligned}
 &\leq \alpha_q \beta_q + \frac{1}{2} \sum_{i=1}^{n-1} \alpha_i^2 + \beta_i^2 \\
 &= \alpha_q \beta_q + \frac{1}{2} (1 - \alpha_q^2) + \frac{1}{2} (1 - \beta_q^2) \\
 &= 1 + \alpha_q \beta_q - \frac{1}{2} \alpha_q^2 - \frac{1}{2} \beta_q^2
 \end{aligned}$$

□

Note that on the domain $\alpha_q \in [-1, 0], \beta_q \in (0, 1]$ the function $1 + \alpha_q \beta_q - \frac{1}{2} \alpha_q^2 - \frac{1}{2} \beta_q^2$ is bounded above by 1 and decreasing to $-\frac{1}{2}$ as $\alpha \rightarrow -1$. Hence, the smaller $\text{CosSim}(\bar{k}, q) = \alpha_q$ is, the smaller $\text{CosSim}(\bar{k}, k^*)$ must be.

Table 7: Resource unrestricted LongBench Results (Higher is better). All methods processes the input prompt in parallel (i.e., block size = ∞) and make an eviction decision with all token information in the input. The token eviction is made at every step of generation if the budget exceeds. We highlight the methods showing the best performance within a given budget with **boldface**. We omit NarrativeQA from evaluation due to higher chance of OOM errors.

Single Doc. QA				Multi Doc. QA				Summarization				Fewshot Learning				Synthetic				Code				Code															
Qasper		MF-en	MF-zh	HopOnQA		2WIKIMQA		Musique		DuReader		GovReport		QMSum		MultiNews		VCSum		TREC		TriviaQA		SAMSum		LSHT		PCount		PR-en		PR-zh		Lcc		RB-P		Avg.	
Llama3.1-8B	47.00	56.12	59.86	57.33	47.81	32.25	35.64	34.86	25.32	27.02	17.28	73.00	91.61	43.37	45.50	8.33	99.50	99.00	61.66	51.94	50.72																		
H2O	2K	22.75	32.73	25.93	43.56	29.49	0.00	5.35	3.70	4.73	17.42	4.44	46.19	54.88	10.39	12.20	16.13	100.00	37.75	42.44	16.44	26.33																	
	4K	35.49	43.14	39.80	52.82	36.60	10.00	6.11	9.34	7.54	24.61	7.38	54.31	65.83	23.18	16.67	16.39	100.00	61.50	55.96	28.68	34.77																	
	6K	44.05	47.74	47.88	52.67	45.90	11.11	7.97	15.55	13.77	26.58	9.13	60.11	78.42	32.35	13.64	12.04	100.00	94.00	60.23	39.82	40.65																	
	8K	45.93	51.12	55.72	53.09	48.83	13.58	15.63	25.89	17.39	27.18	12.39	67.71	86.91	40.05	13.33	13.73	100.00	99.00	60.82	45.17	44.67																	
TOVA	2K	44.37	55.47	58.07	59.16	48.26	16.67	26.58	30.54	24.37	26.81	16.66	71.00	91.93	45.29	28.89	9.84	100.00	96.58	61.65	51.83	48.20																	
	4K	46.45	56.23	58.82	60.72	49.96	15.28	29.93	33.52	25.56	27.18	17.40	91.40	44.49	29.43	13.06	100.00	99.00	61.95	52.19																			
	6K	46.66	54.26	59.31	55.99	50.26	16.22	34.54	34.35	25.21	27.22	17.34	72.96	91.56	44.82	30.43	14.72	100.00	99.00	62.18	53.33	49.52																	
	8K	46.57	53.44	59.16	59.87	51.77	13.58	35.28	35.21	25.98	27.27	16.80	73.23	90.70	44.71	34.78	13.59	100.00	99.00	61.96	54.32	49.96																	
Sink	2K	33.33	33.74	34.73	45.37	38.46	20.97	18.31	26.08	21.41	24.98	16.08	67.50	90.00	40.99	21.25	2.50	36.00	18.00	57.08	53.81	35.03																	
	4K	38.57	41.15	46.38	48.07	40.87	22.51	17.50	25.12	21.89	25.12	16.84	71.50	90.52	41.32	24.75	2.50	49.00	22.50	57.94	53.64	38.09																	
	6K	40.41	43.74	52.60	50.08	42.57	22.32	17.71	30.54	22.38	25.25	17.37	72.50	90.77	41.94	26.25	2.50	57.00	21.00	57.14	54.07	39.41																	
	8K	40.53	44.58	54.77	54.77	49.13	20.35	31.35	22.61	25.28	22.61	17.45	72.50	90.77	42.27	27.75	3.00	70.00	20.50	57.13	55.35	40.57																	
SnapKV	2K	45.01	52.53	56.15	57.54	50.17	25.00	32.35	32.99	25.38	27.24	18.14	70.85	89.48	39.71	26.53	15.86	98.57	87.04	60.56	51.92	48.15																	
	4K	46.28	55.05	59.57	55.49	49.70	24.69	35.09	33.78	26.63	27.15	17.48	72.68	90.28	42.59	28.57	13.38	98.08	98.50	61.14	52.05	49.41																	
	6K	46.82	55.83	59.07	59.68	50.27	22.22	35.82	34.89	25.17	27.24	17.51	72.31	90.76	44.31	23.26	14.00	100.00	99.00	62.13	54.43	49.74																	
	8K	46.72	53.33	59.79	57.18	51.51	15.28	34.83	35.28	25.71	27.24	17.40	71.96	90.46	45.08	23.26	10.92	100.00	98.99	61.76	54.80	49.17																	
KEYDIFF	2K	44.58	53.88	53.65	57.40	47.66	14.89	33.44	29.97	25.88	26.95	16.10	72.00	92.27	43.51	31.82	11.38	100.00	95.92	59.26	45.66	47.81																	
	4K	46.05	54.87	57.52	59.04	49.97	13.58	36.51	33.17	29.52	27.12	16.85	73.00	90.13	43.87	31.82	13.28	100.00	97.67	60.57	50.49	49.07																	
	6K	46.61	54.49	59.19	59.70	50.03	12.99	36.04	34.42	26.67	27.27	17.47	73.33	90.94	44.62	33.33	11.83	100.00	99.00	61.29	53.20	49.62																	
	8K	46.55	55.11	59.28	57.48	50.51	13.58	35.01	34.81	25.87	27.22	17.15	72.59	91.22	44.69	27.27	11.20	100.00	99.00	61.95	53.62	49.21																	
Llama3.2-3B	40.23	50.09	55.84	50.69	42.29	26.84	36.24	33.09	24.30	25.21	16.41	72.50	90.11	42.58	34.00	3.00	96.50	20.50	56.22	56.52	43.66																		
	2K	20.21	24.23	18.98	28.28	23.51	9.88	10.40	1.43	4.13	16.14	3.05	48.00	41.36	12.23	16.00	4.81	1.52	0.50	40.16	17.58	17.12																	
	4K	32.58	33.87	35.46	35.29	27.46	17.84	12.25	6.96	9.26	23.10	5.17	56.00	59.11	21.77	13.70	4.95	13.71	7.25	51.49	29.58	24.84																	
	6K	40.23	44.83	52.90	46.13	36.93	11.61	15.57	13.52	13.03	24.44	7.74	63.50	72.81	30.46	12.86	4.76	12.86	63.00	19.00	50.28	39.85	32.76																
	8K	40.86	49.79	56.31	52.91	42.03	14.74	20.79	22.65	17.06	24.77	10.55	70.50	83.55	35.08	15.07	4.04	81.91	22.22	5.88	95.92	18.50	56.14	55.68	41.20														
TOVA	2K	38.22	48.83	54.09	48.08	42.21	14.81	27.89	28.71	23.27	24.94	15.64	70.50	89.47	42.97	22.22	5.88	95.92	22.50	2.50	36.00	18.00	57.08	53.81	35.03														
	4K	40.55	50.77	56.10	54.26	42.68	17.08	31.66	31.09	23.44	25.37	16.00	71.50	89.77	43.00	21.92	5.88	95.50	18.50	56.33	56.52	42.40																	
	6K	40.57	50.12	56.62	52.67	43.12	19.44	34.78	32.91	23.88	25.30	15.87	72.50	89.07	42.73	24.00	4.35	94.97	20.00	56.30	57.38	42.83																	
	8K	40.86	49.13	54.77	49.13	42.38	23.75	30.35	31.35	22.61	25.28	17.45	72.50	90.77	42.27	27.75	3.00	70.00	20.50	57.13	55.35	40.57																	
Sink	2K	38.15	49.58	51.15	48.73	42.04	20.24	33.47	29.13	23.91	25.10	14.47	70.50	88.31	42.28	20.55	4.90	89.00	17.50	55.21	48.73	40.65																	
	4K	40.55	51.38	55.88	51.56	41.88	18.78	35.93	31.63	24.15	25.38	15.80	71.50	89.98	42.55	19.18	4.95	95.85	21.00	55.79	55.55	42.46																	
	6K	40.54	51.04	55.42	51.78	41.71	15.26	36.60	32.89	24.67	25.34	16.32	72.50	90.58	43.19	22.22	5.21	97.42	20.50	55.87	56.28	42.76																	
	8K	40.66	50.93	56.16	53.52	42.07	17.79	37.08	33.31	24.27	25.31	16.00	72.50	89.48	42.52	25.33	5.00	96.46	20.00	56.20	56.80	43.07																	

Table 8: **Full Llama-3.1-8B/3.2-3B-Instruct LongBench Results with $B = 128$ (Higher is better).** We highlight the methods showing the best performance within a given budget with **boldface**. \dagger : A subset of samples were evaluated due to OOM errors (183/200 samples are evaluated).

Single Doc. QA				Multi Doc. QA				Summarization				Fewshot Learning				Synthetic		Code					
Narrative QA		Qasper	MF-en	HopQoA		MF-zh	2WikiMoA	MultiNews		GovReport	QMSum	VCSum		TREC	TriviaQA	SAMSum	LSTH	PCount	PR-en	PR-zh	Lec	RB-P	Avg
Llama3.1-8B	30.05 ⁵	47.00	56.12	59.86	57.33	47.81	32.25	35.64	34.86	25.32	27.02	17.28	7.300	91.61	43.37	45.50	8.33	99.50	99.00	61.66	51.94	49.74	
2K	1.74	21.15	25.33	21.65	26.11	24.15	8.78	5.90	2.17	2.70	16.78	3.97	44.00	29.36	67.42	14.50	2.25	5.88	4.00	40.15	12.14	24.83	
4K	4.07	36.16	36.00	38.02	33.52	32.87	5.68	6.66	5.95	24.09	6.03	55.00	47.65	17.41	18.50	4.00	24.50	31.25	54.85	21.43	24.13	24.83	
H2O	8.52	43.31	46.24	40.03	42.46	21.68	11.85	8.78	26.03	7.82	62.99	7.96	69.50	66.95	33.41	19.50	5.25	45.50	90.00	58.62	29.53	33.35	
6K	13.85	44.94	47.81	56.14	43.64	23.65	11.01	18.78	26.49	9.96	69.50	66.95	33.41	19.50	5.25	62.50	98.67	59.74	36.26	34.80			
8K	22.57	37.26	39.43	36.96	45.74	34.48	14.77	16.98	28.87	21.17	26.95	16.21	62.50	90.73	42.74	18.75	0.00	18.00	32.00	62.68	52.48	34.35	
2K	4K	22.68	44.55	47.87	51.16	46.76	44.54	20.56	22.50	30.95	22.13	26.96	16.75	61.50	90.56	43.27	25.25	3.00	45.50	84.00	61.62	53.40	41.12
6K	24.59	49.53	52.92	45.95	55.09	50.79	44.73	25.07	27.68	32.33	24.10	27.00	16.91	60.50	90.81	43.89	29.00	4.25	67.00	52.99	41.30	41.12	
8K	24.86	46.78	54.83	57.95	54.52	49.00	26.40	31.15	33.44	24.76	27.00	17.33	7.00	91.11	43.29	33.25	6.25	87.00	98.67	61.49	51.79	47.23	
2K	21.83	34.27	29.24	32.82	38.64	29.50	12.59	16.18	28.51	20.51	26.62	15.54	65.00	89.46	42.20	22.25	2.00	25.50	31.00	32.65	49.54	33.78	
4K	22.94	43.01	39.08	46.16	44.04	41.39	19.09	16.54	31.08	21.57	26.78	16.78	62.87	76.05	91.53	29.25	3.00	38.50	62.12	58.84	39.76		
6K	25.41	47.40	52.78	47.39	45.73	49.61	21.90	17.55	32.53	21.30	26.92	16.91	72.00	91.25	43.41	33.75	3.08	52.50	98.00	62.20	43.49		
8K	23.53	46.63	48.68	55.77	55.47	47.16	21.14	19.54	33.10	23.20	26.92	16.91	72.00	91.29	43.79	37.00	3.25	66.00	99.00	62.18	56.13	44.91	
2K	21.81	37.22	37.19	38.29	46.10	35.42	16.53	16.37	29.83	21.05	26.77	16.16	61.00	88.84	42.26	21.75	4.03	51.50	81.17	62.37	51.45	38.45	
4K	24.79	44.22	47.30	50.27	48.49	46.73	20.55	22.04	32.19	24.27	27.46	13.43	53.33	71.50	91.50	43.14	25.00	5.17	89.50	96.67	64.11	50.20	44.65
6K	24.10	45.57	50.44	55.27	53.12	48.41	24.27	27.46	33.43	23.53	26.93	16.84	61.50	92.28	43.58	27.00	5.25	98.00	61.32	52.16	46.65		
8K	25.15	46.55	53.39	57.65	56.00	48.75	27.82	32.66	33.67	24.85	27.01	17.37	72.50	91.78	43.54	33.75	5.08	100.00	98.67	61.45	51.41	48.05	
2K	8.66	36.63	41.70	37.72	33.75	32.25	5.93	17.73	19.64	14.96	22.69	11.02	63.00	58.94	37.00	22.50	3.05	17.75	20.13	52.40	25.63	10.14	
4K	15.38	44.06	51.75	47.52	50.22	45.56	18.44	22.27	26.93	13.44	26.94	15.12	70.00	86.89	37.50	27.00	4.50	58.00	88.32	35.08	40.14		
6K	21.75	45.63	55.06	53.77	52.93	47.70	25.63	32.66	24.85	22.30	26.94	15.89	71.50	89.26	41.34	34.50	5.25	75.00	98.00	60.98	43.14	45.17	
8K	25.12	45.70	56.02	56.02	56.02	48.14	27.77	33.81	34.09	24.89	26.94	16.81	60.50	90.26	41.34	39.00	7.25	87.00	99.00	61.45	48.05		
2K	26.64	41.73	50.99	51.18	58.51	58.19	46.47	22.84	32.37	29.02	23.86	26.76	14.81	66.50	89.52	42.26	3.17	45.00	96.25	59.17	39.42	45.06	
4K	28.70	45.62	56.06	56.83	54.58	49.31	28.25	33.06	32.30	25.03	27.07	16.32	70.00	90.85	42.84	44.50	4.21	99.00	97.67	60.80	48.00	48.14	
6K	29.90	46.33	55.11	59.00	56.80	49.50	31.52	34.97	33.44	24.58	26.98	16.80	72.00	90.99	43.10	47.00	5.27	99.50	99.00	61.40	46.70	49.19	
8K	33.57	46.77	55.48	57.06	55.48	49.37	30.88	34.54	34.17	25.12	27.01	17.13	72.50	92.28	42.81	46.50	5.83	99.50	98.67	61.48	50.90	49.70	
Llama3.2-3B	23.76	40.23	50.09	55.84	50.69	42.29	26.84	36.24	33.09	24.30	28.21	16.41	72.50	90.11	42.38	34.00	3.00	96.50	20.50	56.22	56.52	42.71	
2K	1.63	19.96	20.20	15.20	18.02	19.56	2.88	6.47	0.78	1.55	15.97	3.11	41.00	21.97	9.83	11.75	0.50	0.00	39.71	13.91	12.60		
4K	3.94	33.23	33.25	23.49	28.08	27.55	10.51	5.44	6.30	22.37	4.81	51.00	38.93	20.23	15.50	1.50	7.50	6.25	22.94	20.28	4.63		
6K	38.81	39.06	45.17	34.66	35.52	15.21	13.36	10.51	10.01	24.25	6.66	61.50	55.23	27.37	15.25	1.50	13.00	19.50	54.55	54.11	36.22		
8K	9.65	39.66	43.20	52.60	38.09	40.41	21.46	18.55	17.80	24.67	13.28	70.00	64.70	32.19	17.00	2.00	24.50	21.50	55.00	39.09	31.15		
2K	17.14	30.14	32.44	31.64	35.96	30.05	13.08	19.62	26.15	19.70	25.04	15.47	56.50	87.81	40.48	16.75	2.50	11.50	52.40	29.36	27.95		
4K	20.52	30.53	42.47	45.80	44.12	38.42	18.22	17.76	20.36	21.36	24.96	16.60	63.50	88.98	41.50	18.75	3.00	23.50	15.00	55.72	56.66		
6K	20.22	39.78	45.86	52.93	49.08	41.54	20.43	24.78	30.50	22.17	26.50	16.37	65.50	89.25	42.20	22.50	4.00	46.50	20.50	55.57	53.75		
8K	21.08	40.67	49.07	51.17	48.69	41.93	23.05	31.02	31.64	22.85	25.21	16.55	69.00	89.25	42.19	22.50	4.00	46.50	20.50	55.57	37.91		
2K	16.85	30.69	27.32	33.26	25.27	13.82	9.38	26.74	19.15	15.88	65.00	86.17	40.93	19.50	1.50	10.50	8.50	56.65	52.73	29.54			
4K	19.46	38.61	36.22	41.68	35.84	13.37	9.86	40.29	29.34	16.64	71.00	88.06	42.04	21.75	2.50	35.50	19.50	56.48	33.96				
6K	19.33	40.29	37.95	44.68	46.48	40.29	11.10	30.43	21.35	25.16	44.11	70.00	88.93	42.04	23.50	3.50	47.00	21.50	55.55	54.11			
8K	20.15	40.02	41.94	53.57	48.15	42.24	16.01	14.76	31.64	22.10	26.98	17.00	73.00	89.26	42.37	26.25	3.50	62.50	21.50	55.55	38.25		
2K	17.38	31.37	31.48	36.96	37.77	30.05	11.54	9.66	27.03	19.93	24.97	15.47	59.00	88.13	40.98	16.25	3.50	32.50	9.00	56.32	55.91		
4K	19.85	39.22	38.96	47.33	46.70	37.08	16.64	16.88	21.21	25.01	16.74	65.50	89.35	41.47	18.75	4.00	85.00	20.00	55.60	55.74			
6K	20.49	40.80	48.16	51.84	49.30	41.65	24.79	20.28	25.32	31.27	23.46	16.81	69.00	90.17	41.99	22.00	5.00	94.00	21.50	55.77	57.29		
8K	20.83	39.65	44.48	48.78	41.65	37.04	20.40	31.40	31.81	24.79	20.28	16.81	69.00	90.17	41.99	22.00	5.00	94.00	21.50	55.77	40.28		
2K	18.29	36.65	45.44	54.77	46.09	35.41	12.79	12.55	21.65	24.86	21.45	12.50	66.50	85.24	37.00	24.88	3.00	49.00	14.00	51.21	40.28		
4K	22.34	40.60	49.15	52.56	50.14	40.30	23.44	21.66	24.46	31.38	23.44	12.50	64.50	85.24	41.41	27.50	2.50	88.50	19.50	55.55	52.44		
6K	22.41	40.77	50.10	54.52	51.74	40.77	23.44	24.83	34.64	42.38	31.53	12.50	65.50	85.24	41.41	27.50	3.00	94.00	21.50	55.86	41.88		
8K	22.41	40.77	50.10	54.52	51.74	40.77	23.44	24.83	34.30	32.78	33.50	12.50	65.50	85.24	41.41	27.50	3.00	94.00	21.50	55.85	42.40		

Table 9: Full Qwen-2.5-7B/3B-Instruct LongBench Results with $B = 128$ (Higher is better). We highlight the best and second best methods within a given budget with **bold** and underline.

Single Doc. QA												Multi Doc. QA												Summarization												Fewshot Learning												Code																																																																																																																																									
Narrative QA			Qasper			MF-en			MF-2h			HypoQA			2WikitMQA			Musique			DbiReader			GovReport			QMSum			MultiNews			VCSum			TREC			TriviaQA			SAMSum			LSHT			PCount			PR-en			PR-2h			Lcc		RB-P		Avg.																																																																																																																												
Qwen2.5-7B	15.75	16.94	32.38	14.87	11.89	11.88	7.95	30.56	34.33	19.91	22.67	15.28	65.50	87.05	44.75	39.47	4.22	93.08	68.79	57.74	61.84	36.04	2K	2.39	7.29	12.42	11.73	8.55	11.06	2.73	6.07	3.62	6.60	15.69	3.44	42.50	28.21	10.63	16.00	0.65	0.00	1.50	35.10	18.77	11.66	11.66	4K	1.99	11.92	19.88	14.72	10.24	4.73	7.51	9.08	10.14	20.85	6.15	51.00	37.37	15.75	3.16	6.43	27.62	52.14	29.09	17.64	17.64	6K	3.34	14.79	22.94	15.33	11.45	11.30	5.52	9.30	14.63	14.27	22.06	8.68	55.75	51.90	18.30	1.39	9.41	54.53	54.68	38.32	22.25	22.25	8K	6.10	15.55	28.29	14.99	12.37	14.65	6.24	16.10	20.78	17.22	22.44	11.12	59.00	58.74	33.05	24.92	1.82	15.73	55.16	55.63	44.56	25.45																																																																							
	12.83	17.03	27.01	14.14	16.80	13.37	8.05	21.15	29.21	19.05	22.73	15.75	56.50	79.56	40.55	20.50	2.43	9.29	20.45	55.99	56.15	23.02		4K	8.49	14.01	21.04	11.55	14.00	11.51	5.09	14.45	27.43	17.84	22.83	15.75	56.50	79.56	40.55	20.50	2.43	9.29	20.45	55.99	56.15	23.02	6K	15.77	15.33	14.58	19.30	25.70	30.40	19.95	22.91	15.10	61.50	83.47	42.90	27.60	1.15	21.75	55.16	57.79	56.59	28.68	28.68	8K	15.69	15.55	33.09	14.78	18.37	13.99	11.26	27.92	31.33	20.17	22.82	15.27	62.00	84.49	43.01	33.21	2.78	30.33	55.16	57.45	58.96	31.79																																																																																															
	14.35	7.68	17.18	23.46	14.65	9.09	9.38	4.39	10.57	30.23	18.62	22.79	15.48	64.50	83.39	44.19	29.81	2.74	18.08	64.95	55.23	51.30	28.46	4K	7.37	16.61	25.73	14.74	11.29	11.27	5.69	11.49	31.47	18.72	22.86	15.62	64.50	84.36	44.47	31.07	3.59	41.38	71.21	55.89	55.99	30.76	6K	8.22	16.15	26.63	15.52	11.59	11.11	6.44	17.29	32.56	18.49	22.91	15.45	65.00	83.95	44.15	35.75	4.14	48.72	71.71	56.82	56.42	31.95	8K	15.60	15.81	33.47	14.77	18.02	14.49	10.53	27.45	31.09	20.09	22.84	15.20	61.00	84.08	43.01	34.28	4.58	64.25	71.71	57.46	60.59	33.56																																																																																													
	14.35	13.45	28.28	13.76	16.33	14.06	8.12	21.96	29.71	19.18	22.82	15.27	50.00	83.80	43.27	35.51	2.41	39.83	55.28	58.12	58.67	30.42	4K	14.34	16.35	31.12	14.16	17.56	14.10	8.74	25.56	31.09	20.16	22.84	15.04	60.00	83.80	42.99	30.81	2.91	54.17	55.16	57.48	60.26	32.32	6K	15.81	15.34	33.47	14.77	18.02	14.49	10.53	27.45	31.09	20.09	22.84	15.20	61.00	84.08	43.01	34.28	4.58	64.25	71.71	57.46	60.59	33.56	8K	14.90	15.77	34.32	14.90	19.02	13.93	9.27	30.65	31.29	20.90	22.79	14.69	60.00	83.01	42.00	38.88	4.13	69.83	54.33	56.76	51.50	32.96																																																																																														
	13.16	12.00	22.28	12.96	12.54	12.38	10.64	7.03	14.40	27.57	18.27	22.85	15.23	58.00	81.78	41.13	23.67	3.76	19.42	35.09	55.83	56.53	26.85	4K	13.42	14.90	35.11	14.15	13.04	13.68	5.39	27.83	25.61	20.42	22.76	13.37	50.00	70.90	40.23	39.62	3.37	58.42	54.86	58.12	55.95	42.27	6K	13.42	14.90	35.11	14.15	18.70	14.09	8.34	30.74	29.83	21.08	22.86	14.39	60.50	77.03	42.00	38.88	4.13	69.83	54.33	56.76	51.50	32.96	8K	14.90	15.77	34.32	14.90	19.02	13.93	9.27	30.65	31.29	20.90	22.79	14.69	60.00	83.01	42.65	40.70	3.87	74.13	55.16	57.33	52.80	33.96																																																																																													
	18.08	22.49	36.72	28.99	27.86	20.45	18.93	32.95	32.80	23.74	24.89	10.95	67.50	85.05	43.88	37.50	5.00	40.97	20.61	51.91	47.53	33.42	4K	1.80	9.18	11.62	12.62	8.54	7.31	2.70	8.57	5.93	6.97	16.89	4.15	38.00	21.87	7.69	16.00	1.00	3.00	2.69	37.36	22.90	11.75	11.75	6K	2.82	17.34	22.27	21.55	10.18	10.47	3.03	11.05	11.06	10.73	22.93	5.77	50.75	34.93	18.03	16.25	4.35	7.32	16.64	47.74	29.42	17.89	17.89	8K	6.16	19.84	32.32	29.66	16.01	17.74	4.26	14.65	14.92	13.89	24.21	7.55	58.00	45.94	24.93	16.00	2.91	9.10	21.32	34.54	21.37	21.37	12K	11.69	14.94	25.33	19.90	17.29	12.58	5.91	15.34	26.67	21.49	24.78	16.58	51.50	68.80	41.79	17.75	0.23	6.00	8.68	49.79	48.60	24.08	14K	12.19	18.31	32.56	27.33	20.58	13.80	7.74	21.11	28.82	22.27	24.98	15.82	59.00	80.66	43.05	21.25	1.11	9.56	19.18	49.93	46.74	27.43	16K	13.62	19.56	34.64	28.72	21.67	16.25	8.47	27.26	30.17	23.10	24.94	16.53	63.50	81.88	42.97	26.25	1.16	10.58	21.32	51.93	50.30	29.03	18K	14.66	20.93	37.77	29.72	22.57	17.08	9.63	29.10	31.12	23.17	24.83	13.48	67.00	84.11	43.55	28.25	2.06	13.08	21.32	51.32	47.64	30.11
	13.75	22.11	20.97	11.63	14.67	4.43	11.89	27.39	19.45	24.36	13.00	56.00	58.77	42.37	22.75	2.50	8.75	4.33	48.27	49.72	23.18	4K	11.46	18.28	30.40	24.02	15.50	14.62	6.97	11.48	30.08	20.12	24.86	13.35	63.00	68.77	43.11	29.50	3.00	11.75	16.75	51.76	50.47	26.63	6K	13.01	20.03	32.59	27.06	18.62	12.70	15.35	30.98	20.70	24.97	13.05	66.50	75.39	42.77	30.00	4.00	14.92	20.44	52.32	50.35	28.39	8K	12.76	20.88	37.10	30.10	22.49	18.19	13.83	29.54	31.33	23.37	24.80	13.75	65.50	84.88	44.49	28.00	5.20	35.83	21.32	51.31	47.82	31.55																																																																																																
	9.71	13.91	24.28	20.75	14.80	10.89	7.42	15.09	27.40	21.63	24.64	15.71	54.50	75.35	42.72	22.38	2.50	18.33	19.06	49.65	50.59	25.87	4K	12.98	22.21	31.77	26.57	18.33	14.41	10.83	21.14	29.14	22.38	24.89	15.88	61.00	84.17	42.63	21.17	3.75	25.52	22.46	50.22	48.77	29.05	6K	14.16	14.16	36.15	28.41	19.14	15.59	12.70	26.21	30.35	22.75	24.91	14.96	65.00	83.92	43.52	25.50	3.00	21.32	21.32	51.04	47.49	36.50	8K	12.24	20.49	38.52	29.60	23.05	19.41	15.95	30.92	31.10	23.89	24.83	11.80	67.50	79.05	41.73	36.50	3.08	40.21	21.32	51.05	45.88	31.82																																																																																														

Table 10: **Llama-3.2-3B-Instruct LongBench Results with prompt block size $B \in [64, 256]$ (Higher is better).** We highlight the best and second best methods within a given budget with **bold** and underline.

Single Doc. QA				Multi Doc. QA				Summarization				Fewshot Learning				Synthetic				Code																	
Narrative QA		Quasar	MF-en	MF-zh		HotpotQA		2WikiQA		Musique		DuReader		QMSum		MultiNews		VCSum		TREC		TriviaQA		SAMSum		LSHT		PCount		PR-zh		Lcc		RB-P		Avg.	
$B = 64$	23.76	40.23	50.09	25.84	50.69	42.29	26.84	36.24	24.30	33.09	24.30	25.21	16.41	72.50	90.11	42.58	34.00	3.00	96.50	20.50	56.22	56.52	42.71														
	2K	1.30	18.23	16.96	14.25	12.26	16.84	0.72	6.88	0.78	1.29	16.24	2.97	35.00	18.07	9.78	13.50	0.50	1.50	0.25	39.98	12.68	11.43														
$H2O$	2K	2.30	31.92	31.59	32.44	25.02	22.58	4.89	9.29	5.36	5.57	23.02	4.80	50.50	33.05	18.76	13.75	1.00	2.50	3.75	50.11	21.57	18.75														
	4K	3.12	38.87	37.63	44.58	35.35	12.13	12.82	10.43	24.31	6.63	63.00	45.46	26.08	14.25	16.27	14.25	17.50	53.84	30.66	25.19																
$H2O$	6K	8K	9.11	40.09	45.04	30.55	12.58	39.24	38.25	17.82	17.97	12.96	24.70	9.26	70.50	60.57	32.71	16.00	0.50	21.50	19.50	7.72	39.26	30.39													
	2K	17.24	30.03	31.04	32.07	36.58	28.97	12.17	10.50	26.35	19.78	25.07	15.20	60.50	87.45	41.07	15.50	1.00	10.50	6.00	55.30	52.36	29.27														
$T0VA$	2K	4K	19.59	39.27	42.16	44.54	44.58	37.63	18.62	17.44	28.82	21.46	16.49	62.50	89.48	41.89	17.50	3.50	24.00	15.00	55.14	56.58	34.35														
	6K	8K	21.32	40.87	50.20	54.35	52.81	49.44	40.35	18.73	24.52	30.71	31.60	22.30	30.47	25.23	16.23	66.00	90.50	41.80	23.25	5.50	74.50	19.50	55.45	58.34	31.64										
$Sink$	2K	15.68	29.91	26.61	27.42	33.16	9.37	26.70	19.25	25.01	16.04	64.50	86.33	41.04	19.00	1.50	19.00	8.50	56.48	52.91	29.39																
	4K	19.35	37.77	36.91	41.61	41.46	35.26	12.88	10.30	29.59	20.27	25.01	16.09	69.00	88.06	41.88	21.25	2.50	36.00	16.50	55.85	52.51	33.81														
$SnapKV$	2K	4K	19.36	38.16	38.16	45.97	46.39	39.01	14.20	30.54	21.64	25.07	16.93	71.00	88.50	42.09	23.50	3.50	47.50	19.50	56.02	53.97	30.36														
	6K	8K	20.49	38.99	42.21	53.08	53.08	41.44	16.37	15.08	31.80	22.04	25.07	16.89	72.00	89.26	42.25	23.50	6.50	19.50	20.50	56.21	56.42	38.04													
$KeyDiff$	2K	18.07	31.21	30.60	31.32	37.31	30.69	11.71	9.98	26.98	19.87	25.13	16.05	61.00	87.85	40.36	16.25	3.00	32.00	8.00	56.78	55.77	30.95														
	4K	19.30	39.01	40.81	44.86	47.83	37.74	16.75	16.94	29.90	21.37	25.25	16.70	65.00	88.88	40.99	16.75	3.50	59.50	18.00	55.15	55.15	31.64														
$KeyDiff$	6K	8K	20.85	41.10	47.89	50.70	48.49	41.79	21.58	31.46	32.03	33.22	23.32	25.12	16.71	66.50	90.00	41.49	18.25	4.49	41.85	18.50	55.46	57.30	30.96												
	2K	17.40	38.12	45.25	47.09	45.28	34.23	13.97	13.97	27.96	28.34	21.09	24.94	13.45	56.00	83.29	38.53	24.25	1.00	63.50	12.50	54.41	40.00	34.79													
$T0VA$	2K	22.38	42.00	50.84	53.16	47.34	40.56	21.43	32.82	30.96	23.32	25.08	15.35	67.50	87.09	42.53	27.50	2.00	89.00	18.50	54.39	53.09	40.33														
	4K	22.25	41.55	50.32	54.91	51.61	42.02	24.62	34.60	32.40	23.63	23.63	23.67	25.21	71.00	88.42	41.90	23.50	3.50	95.00	19.50	55.69	55.77	41.85													
$Sink$	2K	21.57	41.24	50.12	55.33	49.81	43.78	27.45	34.30	34.30	23.63	23.67	23.67	25.21	71.00	88.42	42.32	23.50	3.00	96.50	19.50	55.54	56.56	42.23													
	4K	23.76	40.23	50.09	25.84	50.69	42.29	26.84	36.24	33.09	24.30	25.21	16.41	72.50	90.11	42.58	34.00	3.00	96.50	20.50	56.22	56.52	42.71														
$T0VA$	2K	1.87	19.19	23.35	33.28	32.36	28.34	8.61	10.83	5.46	6.27	23.13	4.98	54.00	41.73	19.14	15.00	1.00	8.00	6.50	51.39	24.24	20.87														
	4K	5.58	31.49	33.28	44.71	44.71	36.18	15.46	13.87	10.77	10.46	24.60	6.94	61.50	32.70	27.20	15.00	1.00	15.00	19.00	54.30	32.35	27.34														
$SnapKV$	2K	9.92	39.71	43.84	52.15	39.14	32.21	19.28	18.04	13.60	24.98	8.99	71.00	67.64	32.83	17.25	2.50	30.00	21.00	55.25	33.33	21.59															
	4K	20.36	38.18	42.53	46.18	46.83	36.60	17.81	17.99	28.99	20.54	25.23	16.34	63.50	89.13	41.55	19.12	3.50	29.50	14.50	55.55	55.91	34.71														
$T0VA$	6K	20.71	40.46	45.82	54.82	50.12	40.71	21.47	30.85	31.47	22.98	25.49	16.41	67.00	88.50	41.90	22.25	2.00	76.50	20.00	55.85	56.74	37.91														
	8K	20.84	40.79	49.02	54.82	50.12	40.71	21.47	30.85	31.47	22.98	25.49	16.41	67.00	88.00	41.79	22.05	2.00	76.50	20.00	55.85	56.74	37.91														
$Sink$	2K	15.48	30.74	26.93	27.76	33.86	25.63	13.30	9.96	26.70	19.41	25.15	15.56	66.00	86.44	41.17	18.50	1.00	19.00	8.50	56.47	52.37	29.50														
	4K	18.91	38.38	37.28	41.76	41.81	35.17	13.07	9.96	29.23	20.61	25.01	16.38	70.50	88.06	42.07	21.75	1.50	36.00	17.00	56.05	51.98	33.93														
$SnapKV$	2K	18.99	37.20	46.57	46.61	45.14	33.12	15.15	29.54	28.30	21.92	25.41	14.44	58.50	86.30	37.77	23.75	1.00	67.00	13.50	54.07	41.59	35.52														
	4K	19.67	39.34	40.95	45.81	44.27	38.78	16.17	16.61	29.99	21.15	25.49	16.71	66.50	89.15	40.76	19.75	3.50	66.00	19.00	55.44	56.65	36.74														
$T0VA$	6K	22.98	40.13	44.80	52.39	50.20	39.28	24.31	24.84	24.84	22.17	25.42	16.55	70.00	89.79	41.91	19.75	3.50	86.50	20.00	55.95	57.49	37.91														
	8K	22.24	40.83	50.23	44.70	54.77	49.74	24.74	31.19	31.95	22.17	25.45	16.27	70.50	90.17	42.12	23.25	4.00	93.50	21.00	55.95	57.36	41.23														

Table 11: **KEYDIFF + Recent tokens Llama-3.1-8B/3.2-3B-Instruct LongBench Results with $B = 128$ (Higher is better).** We highlight the methods showing the best performance within a given budget with **boldface**. X% indicates X% of KV cache budget is reserved to keep the recent tokens, while the remaining cache budget is managed by KEYDIFF algorithm. †: A subset of samples were evaluated due to OOM errors (183/200 samples are evaluated).

		Single Doc. QA		Multi Doc. QA										Summarization						Fewshot Learning				Synthetic			Code	
				Narrative-QA	Qasper	MF-en	MF-zh	HopoutQA	2WikiMQA	Musique	DuReader	GovReport	QMSum	MulitNews	VCSum	TREC	TriviaQA	SAMSum	LSHT	PCount	PR-zh	Lec	RB-P	Avg.				
Llama3.1-8B	30.05 [†]	47.00	56.12	59.86	57.33	47.81	32.25	35.64	34.86	25.32	27.02	17.28	73.00	91.61	43.37	45.50	8.33	99.50	99.00	61.66	51.94	49.74						
	2K	21.83	34.27	29.24	32.82	38.64	29.50	12.59	16.18	28.51	20.21	26.62	15.54	65.00	89.46	42.20	22.25	2.00	25.50	32.50	64.95	59.54	33.78					
	4K	22.94	43.01	39.08	46.16	44.04	41.39	19.09	16.54	31.08	21.57	26.78	16.73	70.00	91.53	42.29	29.25	3.00	38.50	71.00	62.12	58.84	39.76					
	6K	25.41	47.40	44.13	52.78	47.39	45.73	21.90	17.55	32.53	22.19	26.87	17.05	72.00	91.25	43.41	33.75	3.08	52.50	98.00	62.22	56.24	43.49					
Sink	8K	23.53	46.63	48.68	55.77	49.61	47.16	21.14	19.54	33.10	23.20	26.92	16.91	72.00	91.29	43.79	37.00	3.25	66.00	99.00	62.18	56.43	44.91					
	2K	21.81	37.22	37.19	38.29	46.10	35.42	16.53	16.37	29.83	21.05	26.77	16.16	61.00	88.84	42.56	21.75	4.03	51.50	81.17	62.37	51.45	38.45					
	4K	24.79	44.22	47.30	50.27	48.49	46.73	20.55	22.04	32.19	22.68	26.95	16.95	67.50	90.98	43.14	25.00	5.17	89.50	96.67	61.44	51.20	44.46					
	6K	24.10	45.57	50.44	55.27	53.12	48.41	24.27	27.46	33.43	23.53	27.03	16.84	71.50	92.28	43.58	27.00	5.25	98.00	99.00	61.32	52.16	46.65					
SnapKV	8K	25.15	46.55	53.39	57.65	56.00	48.75	27.82	32.66	33.67	24.85	27.01	17.37	72.00	91.78	43.54	33.75	5.08	100.00	98.67	61.48	51.41	48.05					
	2K	27.36	40.79	50.63	50.21	49.44	44.77	25.04	30.25	29.41	23.28	26.76	15.78	64.00	85.90	43.76	44.00	4.25	98.50	95.83	62.97	48.70	45.79					
	4K	27.42	45.67	55.62	57.40	53.77	47.30	27.48	31.90	24.18	24.83	26.83	16.51	70.00	88.89	43.95	47.00	5.21	99.00	98.67	62.20	52.98	48.26					
	6K	30.58	46.24	55.58	57.82	56.44	47.74	29.03	34.33	31.15	24.67	26.91	16.98	71.50	92.22	43.96	47.00	4.23	99.50	99.00	62.36	52.98	49.16					
Recent Tokens	8K	32.17	46.66	55.65	58.65	57.24	48.64	30.54	33.44	33.85	24.93	26.94	17.12	72.00	91.72	43.70	46.00	5.47	99.50	99.00	62.26	51.75	49.43					
	2K	26.73	41.88	49.79	48.46	49.68	42.51	26.90	30.90	28.83	23.34	26.76	16.11	62.50	87.39	43.99	42.50	4.58	94.00	95.58	63.33	50.01	45.51					
	4K	26.05	45.11	55.51	55.87	54.14	47.41	25.52	33.51	31.87	24.40	26.95	16.09	69.00	83.76	43.50	43.50	4.00	99.50	98.67	62.06	52.27	47.92					
	6K	28.39	46.43	55.12	58.27	57.02	48.94	28.98	34.31	33.32	24.62	26.96	17.20	71.20	91.72	44.02	46.50	5.13	99.50	99.00	62.39	52.57	49.14					
KeyDiff + 10%	8K	31.35	46.74	54.71	58.60	58.19	48.14	31.77	34.02	33.55	31.27	24.98	17.11	72.00	91.72	44.17	46.00	7.38	99.50	99.00	62.39	52.04	49.56					
	2K	26.64	41.73	50.99	51.18	51.59	46.47	22.84	32.37	29.02	23.86	26.76	14.81	66.50	85.92	39.26	42.25	3.17	96.00	96.25	59.17	39.42	45.06					
	4K	28.70	45.62	56.06	56.83	54.58	49.31	28.25	32.30	32.30	25.03	27.07	16.32	70.00	90.85	42.84	43.50	4.21	99.00	97.67	60.80	48.00	48.14					
	6K	29.90	46.33	55.11	59.00	58.80	49.50	31.52	34.97	33.44	25.12	27.01	17.13	72.50	92.28	43.10	47.00	5.00	99.50	98.67	61.40	49.70	49.19					
KeyDiff + 20%	8K	33.57	46.77	55.48	59.16	56.87	49.37	30.88	34.54	34.17	25.12	27.01	17.13	72.00	91.95	42.81	46.50	5.83	99.50	99.00	62.50	56.86	53.82					
	2K	23.76	40.23	50.09	55.84	50.69	42.29	26.84	36.24	33.09	24.30	25.21	16.41	72.50	90.11	42.58	34.00	3.00	96.50	20.50	56.22	56.52	42.71					
	4K	16.85	30.69	26.58	27.32	33.26	25.27	13.82	9.38	26.74	19.15	25.15	15.88	65.00	86.17	40.79	19.50	1.50	19.50	8.50	56.65	52.73	29.54					
	6K	19.46	38.61	36.22	41.68	41.97	35.84	13.37	9.86	29.34	20.19	25.06	16.44	71.00	88.06	41.31	21.75	2.50	35.50	16.00	56.48	52.43	33.96					
Sink	8K	20.15	40.02	41.94	53.57	48.15	42.24	16.01	14.76	31.64	22.10	25.20	16.64	71.50	88.93	42.04	23.50	3.50	47.00	22.50	55.74	56.88	36.73					
	2K	17.38	31.37	31.48	39.66	37.77	30.05	11.54	9.66	27.03	19.93	24.97	15.97	59.00	88.13	40.48	16.25	3.50	32.50	9.00	56.32	55.91	30.85					
	4K	19.85	39.22	39.86	47.33	46.70	37.98	16.64	16.88	29.79	21.21	25.01	16.74	65.50	89.35	40.95	18.25	2.50	62.50	22.50	55.69	57.82	39.52					
	6K	20.49	40.80	48.16	55.44	48.78	41.65	24.79	30.40	31.81	23.46	25.17	16.44	70.00	90.17	41.99	22.00	5.00	94.00	21.50	55.77	57.29	41.92					
SnapKV	8K	20.49	37.58	45.99	46.41	44.24	34.81	15.20	29.22	28.23	22.49	24.99	14.71	59.00	84.08	41.38	24.38	3.00	70.50	15.50	57.49	51.91	36.72					
	2K	19.92	40.79	47.55	52.53	47.79	41.92	20.71	32.83	31.12	23.37	25.07	15.77	67.50	87.47	41.28	25.00	2.50	91.00	20.00	57.14	56.25	40.56					
	4K	21.97	40.70	49.76	52.33	49.09	42.34	25.02	34.95	31.97	25.20	25.21	15.91	71.50	88.17	41.67	26.50	3.50	96.00	20.50	56.80	55.18	41.78					
	6K	23.76	40.56	50.79	54.23	50.54	42.15	24.52	34.33	33.02	23.82	25.20	16.08	73.50	89.67	41.99	29.25	3.00	95.00	20.50	57.05	56.48	42.40					
KeyDiff + 20%	8K	23.65	40.58	49.96	55.71	51.52	44.10	25.95	34.41	32.80	23.77	25.25	15.75	73.50	89.67	41.83	28.75	3.00	96.00	20.50	57.00	56.12	42.37					
	2K	19.27	34.86	45.26	44.94	42.81	34.15	14.27	27.31	28.10	22.13	25.08	14.96	61.50	85.07	41.62	24.17	2.00	71.50	16.00	57.56	53.58	36.48					
	4K	22.56	41.28	48.37	52.00	47.50	42.64	19.64	32.28	31.17	22.83	25.08	15.68	68.50	88.17	41.38	24.25	2.00	90.50	19.50	57.04	55.05	40.35					
	6K	22.88	40.74	50.37	55.02	49.10	42.34	24.52	34.53	31.97	25.20	25.24	16.32	71.50	89.61	41.43	27.00	3.00	95.50	20.50	56.82	55.77	41.86					
Recent Tokens	8K	23.82	40.58	50.02	55.71	51.25	43.64	24.52	34.33	33.02	23.82	25.20	16.08	73.50	89.67	41.99	29.25	3.00	97.00	20.50	57.05	56.48	42.40					
	2K	18.29	36.65	45.44	47.47	46.09	35.41	13.79	28.89	28.16	21.45	24.01	13.56	60.00	85.24	37.00	24.88	1.00	60.50	12.00	54.13	42.01	35.09					
	4K	22.34	40.60	49.15	52.56	50.14	40.30	21.65	32.46	31.38	23.44	25.06	15.28	66.50	87.92	41.41	27.50	2.50	88.50	19.5								